THE SOUZA-AURICCHIO MODEL FOR SHAPE-MEMORY ALLOYS

Diego Grandi

Faculty of Mathematics, University of Vienna, Oskar-Morgenstern-Platz 1, A-1090 Vienna, Austria

Ulisse Stefanelli

Faculty of Mathematics, University of Vienna, Oskar-Morgenstern-Platz 1, A-1090 Vienna, Austria

Abstract. Shape-memory alloys are active materials, their amazing thermo-elecromechanical behavior is at the basis of a variety of innovative applications. Many models have been set forth in order to describe this complex behavior. Among these the so-called Souza-Auricchio model appears as remarkably simple in terms of mechanical assumptions yet accurate in the description of three-dimensional experiments and robust with respect to approximations. Our aim is to survey here the current literature on the Souza-Auricchio model, with a specific focus on modeling.

1. **Introduction.** Shape-memory alloys (SMAs) are usually referred to as *active* materials for considerably large strains can be *activated* by either thermal, mechanical, or magnetic stimuli [37, 74, 47]. At high temperatures SMAs completely recover strains as large as 8% during loading-unloading cycles (note that conventional steels plasticize around 1% strains). This amounts to the so-called *super-elastic* behavior of SMAs. At lower temperatures, deformation are permanent. Still, the specimen can be forced to recover its original shape by a thermal treatment: this is the *shape-memory effect*. Finally, some SMAs are ferromagnetic: completely recoverable strains can be induced by the action of an external magnetic field entailing the so-called *magnetic shape-memory effect*. See Figure 1 for a schematic representation of these three effects

SMAs are metallic alloys: specimens are composed by a collection of one or more adjacent crystals with different orientations. We refer to these as the *single-crystal* and the *polycrystalline* situation, respectively. The complex macroscopic behavior of SMAs is the effect of an abrupt and diffusion-less solid-solid phase transformation between different crystallographic configurations (phases): the *austenite* and the *martensites*. Austenite is mostly cubic and it is energetically favored at high temperatures and low stresses. Martensites are lower symmetry crystallographic variants (tetrahedral, orthorhombic, monoclinic, among others) and are favored at low temperature [46, 47, 48]. By cooling an austenitic sample below some critical temperature each crystals trasforms into martensite and specific variants are chosen in such a way to minimize macroscopic work. This result in the emergence of characteristic microstructures such as *laminates* and *twins* [18]. On the other hand, by applying stress or, in some cases, a magnetic field, a specific martensitic

2010 *Mathematics Subject Classification.* 74C05, 35Q74, 49J40, 80A17, 74F15.

Key words and phrases. Shape-memory alloys, variational modeling, magnetism, plasticity, existence, approximation.

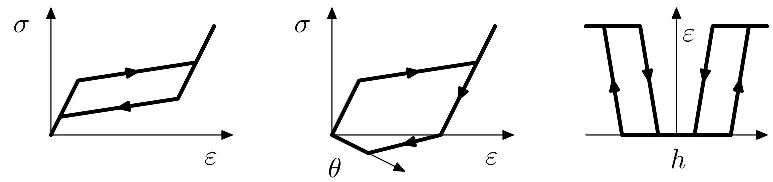

FIGURE 1. Schematic illustration of the super-elastic (left), shape-memory (center), and magnetic effects (right).

variant is preferred with respect to other and to austenite. This triggers a phase transformation which then results in a macroscopic strain affect.

The amazing behavior of SMAs, originally observed in the '60, has attracted enormous attention ever since. The motivation for such an interest is the unprecedented applicative possibilities offered by SMAs. In particular, these are nowadays exploited in a variety of innovative devices including sensors, actuators, MEMS and in a number of different fields from Biomechanics and Medical Engineering, to Seismic and Aerospace Engineering.

The paramount importance of SMAs in applications has triggered an extremely active research activity in the last decades and a whole menagerie of models has been proposed by addressing different alloys (NiTi, CuAlNi, Ni_2MnGa, among the most important) at different scales (atomistic, microscopic with microstructures, mesoscopic with volume fractions, macroscopic) and emphasizing different principles (minimization of stored energy vs. maximization of dissipation, phenomenology vs. rational crystallography and Thermodynamics) and different structures (single crystals vs. polycrystals and structures) [111]. These models have of course ambitions for different ranges of applicability (from lab single-crystal experiments to commercially exploitable tools) and different abilities to fit particular experiments and to explain microstructures, stress/strain relations, or hysteresis. It is beyond our purposes to even attempt a review of the huge literature on these themes. By restricting to the case of macroscopic thermomechanically coupled systems, which are the most relevant for our purposes, we shall however minimally mention the modeling propositions in [8, 9, 53, 56, 73, 105, 106, 107, 108, 125]. From the more mathematical perspective, a distinguished role is played by the *Frémond* model [46, 47, 48] and the *Falk-Konopka* model [43, 44]. These have received extended consideration from the point of view of existence, approximation, and qualitative behavior of solutions. The reader is referred to [25, 29, 30, 49] and [26, 98, 133] and the references therein for a collection of results.

This survey is aimed at reporting on a specific macroscopic model originally proposed by Souza, Mamiya, & Zouain [121] and then combined with finite elements by Auricchio & Petrini [11, 12, 13]. We refer to this as the *Souza-Auricchio* model (SA) in the following. Our interest in the SA model is motivated from one hand by its capability of reproducing the macroscopic behavior of SMAs within a simple variational frame and from the other hand on its amenability to a complete mathematical and numerical discussion. Our survey is intended to highlight the indeed remarkable features of the SA model, to describe its extensions to thermal ferromagnetic and plastic couplings, and to record the available corresponding mathematical results.

By reflecting the progressive development of research of the SA model, this survey is divided into two parts. Sections 2-4 are devoted to the introduction and the mathematical settlement of the SA model in its original isothermal setting. These sections are intended to provide some sequential discussion. Then, the many developments and extensions of the original isothermal theory are collected in Sections 6-9.

2. **Souza-Auricchio model.** The aim of this section is that of introducing the SA model in its original isothermal setting. Reference here are the original papers [11, 12, 13, 121] as well as the mathematical formulation in [10].

2.1. **General features of the SA model.** The SA model is a phenomenological model of *variational type:* the evolution of the state of the material is determined by the specification of the corresponding energy and the choice of the dissipation mechanism. This variational structure allows to frame this model within the by-now classical theory of rate-independent evolutions [81] and, in particular, to discuss existence of solutions, approximations, and discretizations. At the same time, it allows for direct extensions in order to include additional phenomena and features.

The SA model is an *internal-variable-type* model: in the basic isothermal situation the material phase structure is described by a tensorial variable which represent the inelastic strain of the medium. This choice allows for the possibility of accurately describing *reorientation* dynamics in the martensites, that is the passage from one variant to another.

The most striking feature of the SA model is the extremely limited number of material parameters involved. As a matter of example, the full three-dimensional mechanical evolution (isothermal, fully isotropic) requires the specification of just 7 parameters (note that linearized elastoplasticity with linear kinematic hardening already requires 5 parameters). This small number of parameters can be very effectively identified from ordinary uniaxial experiments [16]. Upon this minimal parameter fitting, the SA model has ben proved capable of reproducing well the features of uniaxial and biaxial super-elastic as well as strain-temperature tests.

Before closing this introductory discussion let us also record some drawbacks of the SA modeling perspective. At first, one has to mention the very crude description of unsaturated transformation dynamic (especially the internal structure of hysteresis loops) as well as its simplified tracking of the particular material phases. This lack of detail is to be related with the macroscopic tenet of the SA model.

Additionally, the SA features a strong nonlinear character. This in turn requires a dedicated mathematical and numerical treatment. In particular, the integration of the SA model material description within commercial available finite element codes usually asks for some specific care.

2.2. **Tensor notation.** In the following bold Latin letters stand for vectors and 3-tensors, bold Greek symbols are for 2-tensors, and double-capital letters are for 4-tensors, all of which in $\mathbb{R}^3$. Given the 2-tensors $\boldsymbol{\alpha}$, $\boldsymbol{\beta} \in \mathbb{R}^{3\times3}$, the 3-tensor $\boldsymbol{A} \in \mathbb{R}^{3\times3\times3}$, and the 4-tensor $\mathbb{A} \in \mathbb{R}^{3\times3\times3\times3}$ we classically define $\boldsymbol{\alpha}{:}\boldsymbol{\beta} \in \mathbb{R}$, $\boldsymbol{A}{:}\boldsymbol{\beta}, \boldsymbol{\beta}{:}\boldsymbol{A} \in \mathbb{R}^3$, and $\mathbb{A}\boldsymbol{\beta} \in \mathbb{R}^{3\times3}$ as (summation convention) $\boldsymbol{\alpha}{:}\boldsymbol{\beta} := \alpha_{ij}\beta_{ij}$, $(\boldsymbol{A}{:}\boldsymbol{\beta})_i := A_{ijk}\beta_{jk}$, $(\boldsymbol{\beta}{:}\boldsymbol{A})_i = \beta_{jk}A_{jki}$, and $(\mathbb{A}\boldsymbol{\beta})_{ij} := A_{ij\ell k}\beta_{\ell k}$, respectively. The space of symmetric 2-tensors is denoted by $\mathbb{R}^{3\times3}_{\rm sym}$ and endowed with the natural scalar product $\boldsymbol{\alpha}{:}\boldsymbol{\beta} := {\rm tr}(\boldsymbol{\alpha}\boldsymbol{\beta})$ where ${\rm tr}(\boldsymbol{\alpha}) := \alpha_{ii}$ and corresponding norm $|\boldsymbol{\alpha}|^2 := \boldsymbol{\alpha}{:}\boldsymbol{\alpha}$. Moreover, $\mathbb{R}^{3\times3}_{\rm sym}$ is orthogonally decomposed into $\mathbb{R}^{3\times3}_{\rm sym} = \mathbb{R}^{3\times3}_{\rm dev} \oplus \mathbb{R}\,\mathbf{1}_2$, where $\mathbb{R}\,\mathbf{1}_2$

is the subspace spanned by the identity 2-tensor $\mathbf{1}_2$ and $\mathbb{R}^{3\times 3}_{\rm dev}$ is the subspace of deviatoric symmetric tensors. In particular, for all $\boldsymbol{\alpha} \in \mathbb{R}^{3\times 3}_{\rm sym}$, we have that $\boldsymbol{\alpha} = {\rm dev}\boldsymbol{\alpha} + ({\rm tr}\boldsymbol{\alpha})\mathbf{1}_2/3$.

2.3. **State variables.** Let $\Omega \subset \mathbb{R}^3$ denote the reference configuration of the body and denote by $\boldsymbol{u} : \Omega \to \mathbb{R}^3$ its displacement and by $\theta : \Omega \to \mathbb{R}^+$ its absolute temperature. Moving within the small-deformation polycrystalline regime, we shall additively decompose the linearized strain $\boldsymbol{\varepsilon} = \varepsilon(\boldsymbol{u}) = (\nabla \boldsymbol{u} + \nabla \boldsymbol{u}^\top)/2$ as $\boldsymbol{\varepsilon} = \boldsymbol{\varepsilon}^{\rm el} + \boldsymbol{\xi}$. Here, $\boldsymbol{\varepsilon}^{\rm el} = \mathbb{C}^{-1}\boldsymbol{\sigma} \subset \mathbb{R}^{3\times 3}_{\rm sym}$ corresponds to the elastic part of the strain, $\mathbb{C}$ is isotropic elasticity tensor, and $\boldsymbol{\sigma}$ is the stress. The tensor $\boldsymbol{\xi} \in \mathbb{R}^{3\times 3}_{\rm dev}$ is an internal variable standing for the inelastic strain, also referred to in this context as transformation strain. In particular, $\boldsymbol{\xi}$ is assumed to be trace-free, as experiments suggests that martensitic transformations are approximately isochoric. The quantity $|\boldsymbol{\xi}|$ serves as a measure of the martensitic content of the specimen and fulfills $|\boldsymbol{\xi}| \leq \epsilon_L$ where ϵ_L is the maximal strain which is obtainable by martensitic reorientation. On the other hand, $\boldsymbol{\xi}/|\boldsymbol{\xi}|$ is an indicator of the local orientation of martensites.

In the single-crystal regime we describe the martensitic phase-fraction distribution by the vector $\boldsymbol{p} \in \mathbb{R}^v$ taking values in the simplex

$$S := \{p_i \geq 0, \ p_1 + \ldots + p_v \leq 1\}.$$

The situation $\boldsymbol{p} = \mathbf{0}$ corresponds then to pure austenite whereas $\boldsymbol{p} \in \partial S = \{p_1 + \ldots + p_v = 1\}$ means pure martensite. The corresponding inelastic strain will be given by $\boldsymbol{\xi}(\boldsymbol{p}) = \boldsymbol{\xi}^k p_k$ where $\boldsymbol{\xi}^k$ is the stress-free inelastic strain corresponding to phase k. As a matter of example, we record that in the cubic-tetrahedral system $v = 3$ and a suitable choice for $\boldsymbol{\xi}^k$ is $\boldsymbol{\xi}^k = (3\epsilon_L/\sqrt{6})\,{\rm dev}(\boldsymbol{e}_k \otimes \boldsymbol{e}_k)$ where $\boldsymbol{e}_k$ indicates the k-th coordinate versor.

2.4. **Energy.** The statics of the medium is described by the *Helmholtz free-energy* density

$$\psi = \psi(\boldsymbol{\varepsilon}, \boldsymbol{\xi}, \theta) = c\theta(1 - \log\theta) + \frac{1}{2}(\boldsymbol{\varepsilon} - \boldsymbol{\xi}){:}\mathbb{C}(\boldsymbol{\varepsilon} - \boldsymbol{\xi}) + \frac{1}{2}\boldsymbol{\xi}{:}\mathbb{H}\boldsymbol{\xi} + f(\theta)|\boldsymbol{\xi}| + I(\boldsymbol{\xi}).$$

The parameter $c > 0$ stands for heat capacity density and scales the purely caloric part of the free energy. The quadratic terms in ψ correspond exactly to the free-energy of linearized elastoplasticity with linear kinematic hardening. In particular, $\mathbb{H}$ denotes a suitable fourth-order hardening tensor. The last two terms above are instead characteristic of the SA model. The value $f(\theta)$ corresponds to the martensite-to-austenite equilibrium stress at temperature θ and is measured in MPa. A handy choice (which is however not allowed in the non-isothermal situation, see Section 6) is $f(\theta) = \beta(\theta - \theta_*)^+ = \beta\max\{\theta - \theta_, 0\}$ where θ^* is the martensite-to-austenite transition temperature at zero stress and $\beta > 0$. Finally, $I : \mathbb{R}^{3\times 3}_{\rm dev} \to [0, \infty]$ is the indicator function of the set $\{|\boldsymbol{\xi}| \leq \epsilon_L\}$ that is $I(\boldsymbol{\xi}) = 0$ if $|\boldsymbol{\xi}| \leq \epsilon_L$ and $I(\boldsymbol{\xi}) = \infty$ otherwise. In particular, the constraint $|\boldsymbol{\xi}| \leq \epsilon_L$ is enforced at finite energy.

For the sake of later reference, we can equivalently express the energy of the medium in terms of its *Gibbs free-energy* density as

$$G(\boldsymbol{\sigma}, \boldsymbol{\xi}, \theta) = c\theta(1 - \log\theta) - \frac{1}{2}\boldsymbol{\sigma}{:}\mathbb{C}^{-1}\boldsymbol{\sigma} - \boldsymbol{\sigma}{:}\boldsymbol{\xi} + \frac{1}{2}\boldsymbol{\xi}{:}\mathbb{H}\boldsymbol{\xi} + f(\theta)|\boldsymbol{\xi}| + I(\boldsymbol{\xi}).$$

Both for the Helmholtz and the Gibbs free energy, the single-crystal situation is obtained by replacing $\boldsymbol{\xi}$ by $\boldsymbol{\xi}(\boldsymbol{p})$ and $I(\boldsymbol{\xi})$ by the indicator function $I_S(\boldsymbol{p})$ of the simplex S. Note that we will use the same symbols ψ and G also in the single-crystal case, without introducing new notation.

2.5. **Constitutive equations.** We classically obtain constitutive relations from the variations of the free energie with respect to its variables. In particular, we have that the entropy s, the stress $\boldsymbol{\sigma}$, and the *thermodynamic force* $\boldsymbol{\zeta}$ associated to $\boldsymbol{\xi}$ read

$$s = -\partial_\theta \psi = -f'(\theta)|\boldsymbol{\xi}| + c \log \theta, \tag{1}$$

$$\boldsymbol{\sigma} = \partial_{\boldsymbol{\varepsilon}} \psi = \mathbb{C}(\boldsymbol{\varepsilon} - \boldsymbol{\xi}), \tag{2}$$

$$\boldsymbol{\zeta} = \partial_{\boldsymbol{\xi}} \psi = -\boldsymbol{\sigma} + \mathbb{H}\boldsymbol{\xi} + \beta(\theta - \theta_*)^+ \partial|\boldsymbol{\xi}| + \partial I(\boldsymbol{\xi}). \tag{3}$$

Here and in the following the symbol ∂ corresponds to the subdifferential in the sense of convex analysis. In particular, $\partial|\boldsymbol{\xi}| = \boldsymbol{\xi}/|\boldsymbol{\xi}|$ if $\boldsymbol{\xi} \neq \mathbf{0}$ and $\partial|\mathbf{0}| = \{|\boldsymbol{\xi}| \leq 1\}$ whereas $\partial I(\boldsymbol{\xi}) = \emptyset$ if $|\boldsymbol{\xi}| > \epsilon_L$, $\partial I(\boldsymbol{\xi}) = \mathbb{R}^+ \boldsymbol{\xi}/|\boldsymbol{\xi}|$ if $|\boldsymbol{\xi}| = \epsilon_L$, and $\partial I(\boldsymbol{\xi}) = \mathbf{0}$ if $|\boldsymbol{\xi}| < \epsilon_L$. Note that we could equivalently deduce constitutive relations from the Gibbs energy as $\boldsymbol{\varepsilon} = \partial_{\boldsymbol{\sigma}}(-G)$ and $\boldsymbol{\xi} = \partial_{\boldsymbol{\zeta}}(-G)$.

In the single-crystal case we define the thermodynamic force associated to $\boldsymbol{p}$ as $\boldsymbol{q} = \partial_{\boldsymbol{p}} \psi$. Along with the choice $\boldsymbol{\xi}(\boldsymbol{p}) = \boldsymbol{\xi}^k p_k$ we have

$$\boldsymbol{q} = -\boldsymbol{\sigma}{:}\boldsymbol{E} + \beta(\theta - \theta_*)^+ \partial_{\boldsymbol{p}} |\boldsymbol{\xi}(\boldsymbol{p})| + \mathbb{H}\boldsymbol{\xi}(\boldsymbol{p}){:}\boldsymbol{E} + \partial_{\boldsymbol{p}} I_S(\boldsymbol{p})$$

where $\boldsymbol{E} = \partial_{\boldsymbol{p}} \boldsymbol{\xi}(\boldsymbol{p})$ so that $E_{ijk} = \xi^k_{ij}$.

2.6. **Dissipation and evolution equation.** In order to describe the evolution of the medium we shall prescribe a (pseudo-)potential of *dissipation* $D : \mathbb{R}^{3\times 3}_{\text{dev}} \to [0, \infty)$ of Von-Mises type, namely $D(\dot{\boldsymbol{\xi}}) = R|\dot{\boldsymbol{\xi}}|$ where $R > 0$ is the activation radius. Then, the flow rule consists in the classical normality principle $\partial D(\dot{\boldsymbol{\xi}}) \ni -\boldsymbol{\zeta}$. Indeed, by using also position (3) we obtain the constitutive equation

$$\partial D(\dot{\boldsymbol{\xi}}) + \partial_{\boldsymbol{\xi}} \psi(\boldsymbol{\varepsilon}, \boldsymbol{\xi}, \theta) \ni 0$$

as a generalized balance between the system $\partial_{\boldsymbol{\xi}} \psi$ of the conservative forces and the system ∂D of the dissipative forces. Given the above choices the constitutive relation for the evolution of the material reads

$$R \partial |\dot{\boldsymbol{\xi}}| + \mathbb{H}\boldsymbol{\xi} + \beta(\theta - \theta_*)^+ \partial|\boldsymbol{\xi}| + \partial I(\boldsymbol{\xi}) \ni \boldsymbol{\sigma} \tag{4}$$

In the single crystal setting along with $\boldsymbol{\xi}(\boldsymbol{p}) = \boldsymbol{\xi}^k p_k$ the latter constitutive relations bears the form

$$R \epsilon_L \partial \sum_k |\dot{p}^k| + \mathbb{H}\boldsymbol{\xi}(\boldsymbol{p}){:}\boldsymbol{E} + \beta(\theta - \theta_*)^+ \partial_{\boldsymbol{p}} |\boldsymbol{\xi}(\boldsymbol{p})| + \partial I_S(\boldsymbol{p}) \ni \boldsymbol{\sigma}{:}\boldsymbol{E}. \tag{5}$$

Let us remark once again that the constitutive equation, either (4) or (5), features just 7 material parameters, namely $\mathbb{C}$ (two Lamé constants in the isotropic case), R, $\mathbb{H}$ (one parameter in the isotropic case), β, θ_*, and ϵ_L.

The SA model is dissipative as one directly computes

$$-\dot{\psi} + \boldsymbol{\sigma}{:}\dot{\boldsymbol{\varepsilon}} = (\boldsymbol{\sigma} - \partial_{\boldsymbol{\varepsilon}} \psi \boldsymbol{\sigma}){:}\dot{\boldsymbol{\varepsilon}} - \boldsymbol{\zeta}{:}\dot{\boldsymbol{\xi}} = D(\dot{\boldsymbol{\xi}}) \geq 0$$

for all sufficiently smooth evolutions, and analogously in the single-crystal setting.

2.7. **Illustration of the model behavior.** We shall now comment on how the constitutive relation (4) replicates the super-elastic behavior. In order to check this, let us reduce for the sake of simplicity to the 1D situation. Indeed, we shall consider the reduced 1D constitutive relation

$$R\partial|\dot{\xi}| + H\xi + \beta(\theta - \theta_*)^+\partial|\xi| + \partial I(\xi) \ni \sigma. \tag{6}$$

Assume to be given a sufficiently high temperature so that we are in the super-elastic regime. In particular, let $\theta > R/\beta + \theta_*$ so that $\beta(\theta-\theta_*)^+ = \beta(\theta-\theta_*) > R$. Take $\xi(0) = 0$ and proceed by loading by increasing the stress $t \mapsto \sigma(t)$. Then, $\dot{\xi}$ remains 0 until $\sigma(t) = \beta(\theta-\theta_*)^+ + R$. Afterwards, $\dot{\xi} > 0$ so that, from relation (6),

$$R + H\xi + \beta(\theta-\theta_*)^+ = \sigma.$$

In particular, ξ progressively grows with σ until saturation $\xi = \epsilon_L$.

By unloading from the saturated $\xi = \epsilon_L$ regime one obtains that $\dot{\xi} = 0$ is admissible as long as $\sigma \geq H\epsilon_L + \beta(\theta-\theta_*)^+ - R > 0$. By further unloading the material trasforms again ($\dot{\xi} < 0$) and we reach the nontrasformed case $\xi = 0$ for $\sigma \leq \beta(\theta-\theta_*)^+ - R$. That is, the stress-strain relation is of *play* hysteretic type [26, 128]. In particular, the only value of ξ which is compatible with the stress-free state $\sigma = 0$ is $\xi = 0$. This is exactly the fundamental feature of the super-elastic effect.

The illustration of the shape-memory effect is more subtle. Assume that $\theta < \theta_*$. Then, the constitutive relation (6) in one dimension reads

$$R\partial|\dot{\xi}| + H\xi + \partial I(\xi) \ni \sigma$$

which is nothing but the constitutive relation of linearized elastoplasticity with linear kinematic hardening, at least as long as $|\xi| < \epsilon_L$. In particular, large deformations are not recovered and a loading-unloading cycle may leave a remanent strain even at zero stress. On the other hand, by rising θ enough we have already proved that the only admissible strain at zero stress is $\varepsilon = \xi = 0$. In other words, by heating the medium we restore the initial shape.

The above described material response is very schematic. Still, let us mention that one can easily extend the model in order to capture more detailed features such as nonsymmetric behaviors in tension and compression as well as transformation-dependent materials parameters [16].

2.8. **Relations with other models.** As already mentioned in the Introduction, the macroscopic modeling of SMAs has attracted much research in the last decades a number of models have been set forth. We do not attempt here to review the corresponding huge literature but rather concentrate on outlining the main differences between the SA and some other modeling perspectives.

A classical reference model for SMAs is that of Frémond [46, 47] which has been proved to be amenable to a quite comprehensive mathematical discussion [25, 29, 30, 49, 123]. The crucial difference between the SA and the Frémond model relies in the description of the martensitic structure. Frémond's model is grounded on a *mixing* ansatz on free energies, basically available for an arbitrary number of martensitic variants. Still, the corresponding analysis has been restricted to the consideration of two martensitic variants only. When only two variants are present, one can perform an elementary change of variables in the free energy in order to make the thermomechanical coupling term bilinear. The drawback for this is that the phase descriptor is a scalar and the description of martensite reorientation is out of reach. The SA model instead features a *tensorial* description of the material phase making the description of reorientation amenable. Note that, the interpretation of energy as a mixing is still available for the SA model, see [116].

The tenet of the Falk [43] and the Falk-Konopka [44] models is that the SMA behavior originates by the specific the nonconvexity of the mechanical energy landscape and that internal-variable evolution is viscous. This line of thought has been successfully followed in a series of papers on thermoviscoelasticity for SMAs [19, 20, 33, 78, 79, 98, 103, 133, 134]. On the contrary, the mechanical part of the energy of the SA model is indeed convex and the complex SMA behavior stems from the interaction of energy and rate-independent dissipation instead. This amounts to an enhanced robustness of the modeling with respect to approximations and discretizations, see [10].

In [99, 100, 101, 102] one assumes that the thermomechanical coupling term in the free energy is linear in the temperature θ. This is particularly convenient as it results in the uncoupling of thermal and mechanical variables in the internal energy. This uncoupling however seems not to pair well with the specific case of SMAs.

Eventually, we shall mention that viscous elastic terms, possibly also viscous internal-variable dynamics, albeit disputable form the modeling viewpoint are very often considered in relation with three-dimensional SMA problems. One can check, with no claim of completeness [1, 2, 17, 20, 58, 50, 114] for a collection of existence results.

3. **Quasistatic evolution.** Let us proceed by recording in this section some variational setting for quasistatic evolution. Assume the reference configuration $\Omega \subset \mathbb{R}^3$ to be nonempty, open, connected, and Lipschitz. We decompose the boundary Γ as $\Gamma = \Gamma^{\rm D} \cap \Gamma^{\rm tr}$ where $\Gamma^{\rm D}$ and $\Gamma^{\rm tr}$ are disjoint and $\Gamma^{\rm D}$ has positive surface measure. We define the cylinders $\Omega_T = \Omega\times(0,T)$, $\Gamma_T = \Gamma\times(0,T)$ and so on.

In the isothermal case, we shall be confronted with the quasistatic equilibrium relations coupled with the material constitutive relation as

$$\nabla\cdot(\mathbb{C}\boldsymbol{\varepsilon}(\boldsymbol{u}){-}\boldsymbol{\xi}) = \boldsymbol{0} \quad \text{in } \Omega_T, \tag{7a}$$

$$R\partial|\dot{\boldsymbol{\xi}}| + \mathbb{H}\boldsymbol{\xi} + \beta(\theta{-}\theta_*)^+\partial|\boldsymbol{\xi}| + \partial I(\boldsymbol{\xi}) + \partial V(\boldsymbol{\xi}) \ni \mathbb{C}(\boldsymbol{\varepsilon}(\boldsymbol{u}){-}\boldsymbol{\xi}) \quad \text{in } \Omega_T, \tag{7b}$$

$$\boldsymbol{u} = \boldsymbol{0} \quad \text{in } \Gamma^{\rm D}_T, \quad \boldsymbol{\sigma}\boldsymbol{\nu} = \boldsymbol{g} \quad \text{in } \Gamma^{\rm tr}_T \tag{7c}$$

$$\boldsymbol{\xi}(0) = \boldsymbol{\xi}^0 \quad \text{in } \Omega. \tag{7d}$$

Here $\boldsymbol{\nu}$ stands for the outward unit normal to Γ and $\boldsymbol{g} : \Gamma^{\rm tr}_T \to \mathbb{R}^3$ is a given traction at the boundary (we could consider also some body force in (7a) with no particular intricacy). The functional V represents a suitable differential operator. Choices for V are

$$V_1(\boldsymbol{\xi}) = \frac{\kappa}{2}\int_\Omega |{\rm D}\boldsymbol{\xi}|^2, \quad V_2(\boldsymbol{\xi}) = \kappa\int_\Omega |{\rm D}\boldsymbol{\xi}|, \quad V_3(\boldsymbol{\xi}) = \frac{1}{2}\int_\Omega \mathbb{K}(x,y)\boldsymbol{\xi}(x){:}\boldsymbol{\xi}(y){\rm d}x\,{\rm d}y \tag{8}$$

for $\kappa > 0$ and $\mathbb{K} \in L^1(\Omega\times\Omega;\mathbb{R}^{3\times3\times3\times3})$. Correspondingly, the symbol ∂V has to be interpreted here as the (density of the) variational derivative of V, namely

$$\partial V_1(\boldsymbol{\xi}) = -\kappa\Delta\boldsymbol{\xi}, \quad \partial V_2(\boldsymbol{\xi}) = -\kappa\nabla\cdot\left(\frac{\nabla\boldsymbol{\xi}}{|\nabla\boldsymbol{\xi}|}\right), \quad \partial V_3(\boldsymbol{\xi})(x) = \int_\Omega \mathbb{K}(x,y){:}\boldsymbol{\xi}(y){\rm d}y.$$

All the above functionals V bear a compactifying effect (for $\mathbb{K}$ suitably singular at $x = y$) and introduce a length scale in the model, to be compared with typical sizes of martensitic structures. The first quadratic functional gives rise to an easily handled linear laplacian term in (7c) and, as such, is often encountered in this context. One has however to notice that the choice of V to be quadratic entails the emergence of diffusion and transition layers and calls for the specification of boundary conditions on $\boldsymbol{\xi}$. All these issues are usually regarded as troublesome for SMAs. On the contrary, the second *total variation* functional still penalizes martensitic interfaces. However it does not prevent $\boldsymbol{\xi}$ from possibly exhibiting jumps. This is a particularly desirable feature in connection with shape-memory alloys where few-atoms-thick martensitic-phase structures are observed. The advantage of the third choice V_3 is that it does not require the specification of boundary conditions, an often disputed instance.

4. **Existence and approximations.** One of the crucial features of the SA model is its amenability to approximations and discretizations. This in turn entails the possibility of devising existence results, either at the level of material points and at the three-dimensional level of quasistatic evolution. Evolution within the SA model can be reformulated in the energetic sense, following Mielke & Theil [91]. We shall minimally review the existence theory for energetic solutions in Subsection 4.1 and record the related results for the SA model in Subsection 4.2 and 4.3, for the constitutive relation and the quasistatic evolution, respectively. Eventually, we comment on space-discretizations in Subsection 4.5 and on general approximation issues in Subsection 4.4.

4.1. **Energetic solutions.** We present a minimal aside on the existence theory for energetic solutions, leaving all proofs, detail, and generalization to the papers [91, 81]. We shall be concerned with the evolution of a state $t \in [0,T] \mapsto q(t) \in Q$ where Q is a suitable Banach space. We assume to be given an energy $E : [0,T]\times Q \to \mathbb{R}$ and a positively 1-homogeneous dissipation $D : Q \to [0,\infty]$. The evolution of q starting from some given initial state q^0 follows the rate-independent flow

$$\partial D(\dot{q}(t)) + \partial_q E(t, q(t)) \ni 0 \quad \text{for } t \in (0,T), \quad q(0) = q^0. \tag{9}$$

We shall focus on a suitable weak formulation of the latter by saying that $t \mapsto q(t)$ is an *energetic solution* of (9) if $q(0) = q^0$ and, for all $t \in [0,T]$,

$$q(t) \in S(t) = \{q \in Q \;\; E(t,q) \le E(t,\widehat{q}) + D(\widehat{q}-q) \;\; \forall \widehat{q} \in Q\}, \tag{10}$$

$$E(t,q(t)) + \mathrm{Diss}(q;[0,t]) = E(0,q^0) + \int_0^t \partial_s E(s,q(s))\mathrm{d}s. \tag{11}$$

Here $\mathrm{Diss}(q;[0,t])$ corresponds to the supremum of $\sum D(q(t_i) - q(t_{i-1}))$ over partitions $\{0 = t_0 < t_1 < \cdots < t_N = t\}$. The inclusion $q(t) \in S(t)$ is usually called *global stability* whereas (11) is nothing but *energy conservation*. The advantage of dealing with energetic solutions consists in reducing to a system of a *static* variational inequality (10) coupled with a *scalar* equation (11) instead of the *evolutionary* variational inequality (9). A second remarkable advantage of the energetic formulation is that of being gradient-free, both for the functionals and the solution. This is particularly convenient for nonsmooth situations. We shall recall that the system (10)-(11) (along with the initial condition) is equivalent to the strong formulation (9) for convex energies (that is, for all cases considered in this section) and weaker in all other cases.

Here and in the following we assume that $E(t,\cdot)$ has compact sublevels for all t, $\partial_t E$ exists and is linearly bounded by E, $\partial_t E(\cdot,q)$ is absolutely continuous for all q, D is convex, continuous, and vanishes just in 0, and that $q^0 \in S(0)$. Then, an energetic solution can be obtained by time discretization by letting $q_0 = q^0$ and solving recursively the incremental minimization problem

$$\min\left(E(t_i, q) + D(q - q_{i-1})\right) \quad \text{for } i = 1, \dots, N \tag{12}$$

where $\{0 = t_0 < t_1 < \cdots < t_N = T\}$. The latter has at least a solution as $q \mapsto E(t_i, q) + D(q - q_{i-1})$ is coercive and lower semicontinuous. In particular, by indicating by $\tau = \max(t_i - t_{i-1})$ and letting q_τ be the right-continuous piecewise constant interpolant of $\{q_0, \dots, q_N\}$ on the partition one has that, up to not relabeled subsequences, $q_\tau \to q$ point-wise in time where q is an energetic solution. Moreover, we have that $\mathrm{Diss}(q_\tau; [0,t]) \to \mathrm{Diss}(q; [0,t])$ and $E(t, q_\tau(t)) \to E(t, q(t))$ for all times.

4.2. **Existence for constitutive relation.** We are interested in the stress-driven evolution in the material point. Namely, given a temperature $\theta > 0$, a sufficiently regular stress history $t \in [0,T] \mapsto \boldsymbol{\sigma}(t)$ and an initial state $\boldsymbol{\xi}^0$, one looks for $t \in [0,T] \mapsto \boldsymbol{\xi}(t)$ solving the constitutive relation (4) such that $\boldsymbol{\xi}(0) = \boldsymbol{\xi}^0$. This can be set in the frame of Subsection 4.1 by letting $q = \boldsymbol{\xi}$, $Q = \mathbb{R}^{3\times3}_{\mathrm{dev}}$, $D(\dot{\boldsymbol{\xi}}) = R|\dot{\boldsymbol{\xi}}|$, and $E(t, \boldsymbol{\xi}) = \boldsymbol{\xi}{:}\mathbb{H}\boldsymbol{\xi}/2 + \beta(\theta - \theta_*)^+|\boldsymbol{\xi}| + I(\boldsymbol{\xi}) - \boldsymbol{\xi}{:}\boldsymbol{\sigma}(t)$ so that $\partial_t E = -\boldsymbol{\xi}{:}\dot{\boldsymbol{\sigma}}(t)$. Hence, one can build a solution to (4) by passing to the limit into time-discretization. In particular, one can define $\boldsymbol{\xi}_0 = \boldsymbol{\xi}^0$ and solve iteratively the backward (implicit) Euler scheme

$$R\partial|\boldsymbol{\xi}_i - \boldsymbol{\xi}_{i-1}| + \mathbb{H}\boldsymbol{\xi}_i + \beta(\theta - \theta_*)^+\partial|\boldsymbol{\xi}_i| + \partial I(\boldsymbol{\xi}_i) \ni \boldsymbol{\sigma}(t_i) \tag{13}$$

for $i = 1, \dots, N$. The latter has a unique solution as it corresponds to the successive minimization of the uniformly convex functionals $\boldsymbol{\xi} \mapsto D(\boldsymbol{\xi} - \boldsymbol{\xi}^{i-1}) + E(t_i, \boldsymbol{\xi})$. For such a minimization one can quite effectively develop suitable *return-map-like* algorithms, in analogy to plasticity. By assuming $\boldsymbol{\sigma} \in W^{1,1}(0,T)$ and $\boldsymbol{\xi}^0 \in S(0)$, and by letting $\boldsymbol{\xi}_\tau$ denote the right-continuous piecewise interpolant of $\{\boldsymbol{\xi}_i\}_{i=0}^N$ on the partition, one gets that $\boldsymbol{\xi}_\tau \to \boldsymbol{\xi} \in W^{1,1}(0,T)$ point-wise and strictly in $BV(0,T)$ where $\boldsymbol{\xi}$ solves (4). The full strain $\boldsymbol{\varepsilon}$ can then be readily reconstructed from relation (2). Analogous considerations can be made in the single-crystal case of (5).

4.3. **Existence for the quasistatic evolution.** Assume to be given temperature $\theta > 0$, a suitable initial value $\boldsymbol{\xi}^0$, and the traction $\boldsymbol{g} \in W^{1,1}(0,T; L^2(\Gamma^{\mathrm{tr}}; \mathbb{R}^3))$. We define $q = (\boldsymbol{u}, \boldsymbol{\xi})$ and

$$Q = \{\boldsymbol{u} \in H^1(\Omega; \mathbb{R}^3) \,:\, \boldsymbol{u} = \mathbf{0} \text{ on } \Gamma_D\} \times \{\boldsymbol{\xi} \in L^1(\Omega; \mathbb{R}^{3\times3}_{\mathrm{dev}}) \,:\, V(\boldsymbol{\xi}) < \infty\},$$

and let $D(\dot{q}) = \int_\Omega R|\dot{\boldsymbol{\xi}}|$ and

$$E(t,q) = V(\boldsymbol{\xi}) + \int_\Omega \left(\frac{1}{2}(\boldsymbol{\varepsilon}(\boldsymbol{u}) - \boldsymbol{\xi}){:}\mathbb{C}(\boldsymbol{\varepsilon}(\boldsymbol{u}) - \boldsymbol{\xi}) + \frac{1}{2}\boldsymbol{\xi}{:}\mathbb{H}\boldsymbol{\xi} + \beta^*|\boldsymbol{\xi}| + I(\boldsymbol{\xi})\right) - \int_{\Gamma^{\mathrm{tr}}} \boldsymbol{g}\cdot\boldsymbol{u}$$

where $\beta^* = \beta(\theta - \theta^*)^+$. The latter choices fit into the frame of Subsection (4.1). In particular, $E(t, \cdot)$ has compact sublevels with respect to the weak$\times$strong topology in Q and D is continuous in L^1. Moreover, the power of external actions $\partial_t E$ is linear in $\boldsymbol{u}$, hence regular. In particular, one can obtain a solution to the quasistatic evolution problem by passing to the limit in the time-discrete problems (12), each of which corresponds to a nonlinear elliptic system.

Before closing this subsection let us remark again the crucial role played by the nonlocal operator V for it entails strong compactness in L^1 for the $\boldsymbol{\xi}$ variable. No existence result for solutions in function spaces is presently available when omitting this compactification.

4.4. **Regularization.** The energy E from Subsection 4.3 is nonsmooth in $\boldsymbol{\xi}$. This nonsmoothness is indeed crucial for the behavior of the model, as illustrated in Subsection 2.7. On the other hand, a smooth energy would allow a simpler analytical and computational treatment. As such, one is brought to the consideration of regularized energies depending on an extra user-defined parameter $\rho > 0$. In particular, one replaces the nonsmooth part $\beta(\theta-\theta^*)^+|\boldsymbol{\xi}|+I(\boldsymbol{\xi})$ by some regularization obtained by penalization and smoothing as, for instance,

$$\phi_\rho(\boldsymbol{\xi}) = \beta(\theta-\theta^*)^+\sqrt{\rho+|\boldsymbol{\xi}|^2} + \frac{1}{2\rho}((|\boldsymbol{\xi}|-\epsilon_L)^+)^2.$$

This regularization does not alter the uniform convexity of the energy. It can be then considered in the spirit of proving continuous dependence on data (and hence uniqueness) of the solutions, both for the constitutive relation (4) and the quasistatic evolution (7a)-(7b), see [10].

On the other hand, the regularization turns out useful in simulations. For instance, the Euler scheme (13) can be the rephrased equivalently as the smooth nonlinear equation

$$\boldsymbol{\xi}_i - \boldsymbol{\xi}^{i-1} = L^{-1}(\boldsymbol{\sigma}(t_i) - \phi_\rho(\boldsymbol{\xi}^i) - \mathbb{H}\boldsymbol{\xi}_i)$$

where $L(\boldsymbol{\xi}) = R\partial|\boldsymbol{\xi}| + \mathbb{H}\boldsymbol{\xi}$ has Lipschitz continuous inverseL^{-1}. Hence, one can tackle the problem with conventional methods.

By taking $\rho \to 0$ the (unique) solutions of the regularized problems converge to solutions of the nonregularized ones ($\rho = 0$) [10]. Moreover, the limit in the regularization parameter ρ commutes with discretization in time. For a general tractation of evolutive Γ-limit issues in rate-independent evolution the reader is referred to [89].

4.5. **Space discretization.** In the 3D case of quasistatic evolution, the time discretization in (12) can be combined with space discretization in order to give rise to a fully discrete scheme. In particular, one can introduce finite-dimensional subspaces $Q_h \subset Q$ exhausting Q and define D_h and E_h to be D and E restricted to Q_h. Under suitable assumptions and for $V(\boldsymbol{\xi}) = (1/2)\int_\Omega |\mathrm{D}\boldsymbol{\xi}|^2$ one can prove that the limit $h \to 0$ gives a solution to the space-continuous problem [85]. More precisely, by denoting by $(\boldsymbol{u}_{h\tau}, \boldsymbol{\xi}_{h\tau})$ the solutions to the fully-discrete and regularized problem (see Subsection 4.4), under additional qualification on the domain Ω and the initial state $\boldsymbol{\xi}^0$, one can find that [86]

$$\|\boldsymbol{u}-\boldsymbol{u}_{h\tau}\|_{H^1} + \|\boldsymbol{\xi}-\boldsymbol{\xi}_{h\tau}\|^2_{L^2} \le C(h^{\sigma/2} + \tau^{1/2})$$

for some $0 < \sigma < 1$, where $(\boldsymbol{u}, \boldsymbol{\xi})$ solves the continuum problem.

5. **Finite strains.** Martensitic-transformation strains can be as large as 10%. As such, the small-strain assumption may be questionable. Originally proposed in the small-strain regime, the SA has been extended to finite strains in [41, 42] and then reconsidered in [51]. The starting point is the multiplicative decomposition of the deformation gradient $\mathrm{D}\boldsymbol{f} = \boldsymbol{\xi}_{\mathrm{el}}\boldsymbol{\xi} : \Omega \to \mathrm{GL}_+(3) = \{\det \boldsymbol{\alpha} > 0\}$ where $\boldsymbol{f} : \Omega \to \mathbb{R}^3$ is the deformation, $\boldsymbol{\xi}_{\mathrm{el}} \in \mathrm{GL}_+(3)$ is the elastic part and $\boldsymbol{\xi} \in \mathrm{SL}(3) = \{\det \boldsymbol{\alpha} = 1\}$ is

the inelastic part of the deformation gradient [72]. The free-energy density of the medium is given as

$$\psi(\mathrm{D}\boldsymbol{f}, \boldsymbol{\xi}, \theta) = W(\mathrm{D}\boldsymbol{f}\boldsymbol{\xi}^{-1}) + \beta(\theta-\theta_*)^+|\boldsymbol{\eta}| + \frac{H}{2}|\boldsymbol{\eta}|^2 + I(\boldsymbol{\eta})$$

where $\boldsymbol{\eta} = (\boldsymbol{\xi}^\top\boldsymbol{\xi}-\mathbf{1}_2)/2$ is the so-called *Green-St. Venant* tensor and, $H > 0$ is a hardening modulus. Here, W is a polyconvex, isotropic, and frame-indifferent hyperelastic energy. In particular, we can allow for $W(\boldsymbol{\xi}_{\rm el}) \to \infty$ for $\det \boldsymbol{\xi}_{\rm el} \to 0^+$. A possible choice for W is terms of its first and second invariants is proposed in [42].

We can equivalently reformulate the model in terms of the *right Cauchy-Green* deformation tensor $\boldsymbol{\gamma}_{\rm el} = \boldsymbol{\xi}_{\rm el}^\top\boldsymbol{\xi}_{\rm el}$ and its inelastic analogue $\boldsymbol{\gamma} = \boldsymbol{\xi}^\top\boldsymbol{\xi}$ by letting $\psi = \psi_{\rm el} + \psi_{\rm tr}$ where $\psi_{\rm el}(\boldsymbol{\gamma}_{\rm el}) = W(\boldsymbol{\xi}_{\rm el})$ and $\psi_{\rm tr}(\boldsymbol{\gamma}, \theta) = \beta(\theta-\theta_*)^+|\boldsymbol{\eta}| + (H/2)|\boldsymbol{\eta}|^2 + I(\boldsymbol{\eta})$.

By letting $\boldsymbol{\omega}$ denote the *second Piola-Kirchhoff* tensor $\boldsymbol{\omega} = 2\boldsymbol{\xi}^{-1}\partial\psi_{\rm el}\boldsymbol{\xi}^{-\top}$, defining $\boldsymbol{\tau} = \boldsymbol{\xi}^{-1}\boldsymbol{\mu}\boldsymbol{\xi}^{-\top} - \boldsymbol{\alpha}$ where $\boldsymbol{\mu} = 2\boldsymbol{\gamma}_{\rm el}\partial_{\boldsymbol{\gamma}_{\rm el}}\psi_{\rm el}$ is the so-called *Mandel* stress and $\boldsymbol{\alpha} = 2\partial_{\boldsymbol{\gamma}_{\rm el}}\psi_{\rm tr}$ is the *back-stress*, the evolution of the medium is given by the associative flow rule

$$\dot{\boldsymbol{\gamma}} = \dot{\zeta}\partial_{\boldsymbol{\tau}} f(\boldsymbol{\xi}, \boldsymbol{\tau})$$

along with the complementarity conditions $\dot{\zeta} \geq 0$, $f \leq 0$, and $\dot{\zeta} f = 0$. Here, the *yield function* f is given by $f(\boldsymbol{\xi}, \boldsymbol{\tau}) = |\mathrm{dev}(\boldsymbol{\xi}\boldsymbol{\tau}\boldsymbol{\xi}^\top)| - R$ for some yield stress $R > 0$.

Along with the latter flow rule, the model is proved to be dissipative in [51]. In particular, we check that all smooth evolutions fulfill the Clausius-Duhem inequality

$$-\dot{\psi} - s\dot{\theta} + \boldsymbol{\omega}{:}\frac{1}{2}\boldsymbol{\gamma}_{\rm el} - \boldsymbol{q}\cdot\frac{\nabla\theta}{\theta} \geq 0$$

so that the entropy-production rate is nonnegative. The reader is referred to [41, 42] for a computational assessment on the capability of the model and to [51] for a variational reformulation in terms of energetic solutions and an existence and discretization convergence proof for the constitutive relation.

In [41, 42] it is argued that, by considering small deformations, the finite-strain model approaches the original small-strain one. This remark is presently just a point-wise convergence argument for the involved functionals. It would be interesting to develop a rigorous convergence analysis for energetic trajectories in the spirit of the finite-to-inifinitesimal plasticity theory of [90].

6. **Non-isothermal evolution.** While the isothermal regime can be considered to be satisfactory for describing the super-elastic effect, the shape-memory effect is activated by temperature changes instead. To this end, one is clearly obliged to step off the isothermal regime.

6.1. **Given temperature.** When the body is thin in at least one direction and mechanical cycles have a suitably low frequency one can assume that the heat produced in the specimen is immediately transferred to the surrounding environment acting as a heat bath. Hence, by assuming the temperature to agree with a given external temperature $t \mapsto \theta(t) = \theta_{\rm ext}(t)$ for all times, one is interested in considering a quasistatic evolution problem (7). This has been done in [87] and [84] in the polycrystal and single-crystal case, respectively. In both papers, the elasticity tensor $\mathbb{C} = \mathbb{C}(\theta)$ is assumed to be smoothly dependent on θ in order to reflect the different elastic behavior of austenite and martensite. Moreover, the thermoinelastic part of the free energy $f(\theta)|\boldsymbol{\xi}| + I(\boldsymbol{\xi})$ is regularized in both θ and $\boldsymbol{\xi}$, see Subsection 4.4 and well-posedness of the problem is proved in the energetic sense. Some further existence result under weaker assumptions on $\theta(t)$ and no regularization in $\boldsymbol{\xi}$ is reported in [40].

6.2. **Thermodynamic consistency.** In order to include temperature evolution in the model one is forced to complete the quasistatic problem (7) by the entropy balance equation

$$\theta \dot{s} + \nabla \boldsymbol{q} = -\boldsymbol{\zeta}{:}\dot{\boldsymbol{\xi}} = D(\dot{\boldsymbol{\xi}})$$

where $\boldsymbol{q}$ is the heat flux. For the sake of definiteness we now choose the Fourier law $\boldsymbol{q} = -\kappa \nabla \theta$ where $\kappa > 0$ measures thermal conductivity. Along with the above choices we obtain the heat equation

$$(c - \theta f''(\theta)|\boldsymbol{\xi}|)\dot{\theta} - \kappa \Delta \theta = R|\dot{\boldsymbol{\xi}}| + \theta f'(\theta)|\boldsymbol{\xi}|^{\cdot}. \tag{14}$$

to be combined with suitable initial and boundary conditions.

The system (7)+(14) can be proved to be thermodynamically consistent as

$$-\dot{\psi} - s\dot{\theta} + \boldsymbol{\sigma}{:}\dot{\boldsymbol{\varepsilon}} - \boldsymbol{q}\cdot\frac{\nabla\theta}{\theta} = D(\dot{\boldsymbol{\xi}}) + \kappa\frac{|\nabla\theta|^2}{\theta} \geq 0.$$

6.3. **Unknown temperature, 1D.** Note that the original choice $f(\theta) = \beta(\theta - \theta_*)^+$ do not pair well with the computation in (14). This is not a mere matter of regularity but rather a substantial thermodynamical obstruction. Indeed, by inspecting the form of the entropy from (1) one realizes that, given $\boldsymbol{\xi} \neq \boldsymbol{0}$ and fixed, the relation $\theta \mapsto s(\theta)$ is strictly increasing iff $\beta < c$. As this basic requirement need to be fulfilled in order for thermodynamic consistency to be ensured, one is forced to resort to some regularized version of f instead. Even more, from the heat equation (14) one finds that indeed $c - f''(\theta)|\boldsymbol{\xi}|$ serves as an effective heat capacity. This induces a second restriction on the possible choice of f as the relation $c - f''(\theta)|\boldsymbol{\xi}| > 0$ have to be ensured in order to preserve dissipativity (that is, the parabolic nature of the system).

These issues have been analyzed in [67, 68] in the one-dimensional case. In particular, by introducing suitable smallness assumptions on f, it is proved that the system (7)+(14) admits a unique solution. Note that a counterexample to existence when such smallness assumptions are not fulfilled is recorded in [67].

6.4. **Unknown temperature, 3D.** Existence results in three space dimensions for the fully coupled thermomechanical system (7)+(14) are presently not available.

Still, one has to mention some related existence arguments which are obtained by assuming additional smoothness and considering viscosity [99, 100, 101, 102, 103, 113, 117]. These modifications are intended to tame the strongly nonlinear character of the dissipation, see the right-hand side of equation (14). The effect is however that the model substantially deviate from the original SA formulation. In particular, one has to mention that in all of the above contributions, the thermomechanical energy term is assumed to be linear in θ in such a way that thermal and mechanical effects decouple in the internal energy expression. This is not completely satisfactory with respect to the SA model where the thermomechanical coupling is modulated by the nonlinear function f. This linearity ansatz is removed in the recent [115, 116] which will be described in Subsection 9 below.

6.5. **Variational formulation via GENERIC.** Let us present here the possibility of providing a variational formulation of the fully coupled thermomechanical material evolution by resorting to the GENERIC formalism in thermoplasticity from [82, 83]. This possibility is particularly remarkable as it allows to enlighten the gradient structure underlying the full thermomechanical evolution.

Let us preliminarily compute the internal energy e by means of the classical Helmholtz relation

$$e = \psi + \theta s = c\theta + \frac{1}{2}(\boldsymbol{\varepsilon}-\boldsymbol{\xi}){:}\mathbb{C}(\boldsymbol{\varepsilon}-\boldsymbol{\xi}) + \frac{1}{2}\boldsymbol{\xi}{:}\mathbb{H}\boldsymbol{\xi} + \big(f(\theta)-\theta f'(\theta)\big)|\boldsymbol{\xi}| + I(\boldsymbol{\xi}).$$

By restricting to an isolated system, we can introduce the energy, entropy, and dual dissipation functionals as

$$\mathcal{E}(\boldsymbol{u},\boldsymbol{\xi},\theta) = \int_\Omega e(\boldsymbol{u},\boldsymbol{\xi},\theta)\mathrm{d}x, \quad \mathcal{S}(\boldsymbol{\xi},\theta) = \int_\Omega s(\boldsymbol{\xi},\theta)\mathrm{d}x,$$

$$\mathcal{K}^*(\boldsymbol{u},\boldsymbol{\xi},\theta;\boldsymbol{v}_{\boldsymbol{\xi}},\boldsymbol{v}_\theta) = \int_\Omega I_{R/\theta}\left(\boldsymbol{v}_{\boldsymbol{\xi}} - \frac{\boldsymbol{v}_\theta}{\partial_\theta\mathcal{E}}\partial_{\boldsymbol{\xi}}\mathcal{E}\right)\mathrm{d}x + \frac{\kappa}{2}\int_\Omega\left|\nabla\left(\frac{\boldsymbol{v}_\theta}{\partial_\theta\mathcal{E}}\right)\right|^2\mathrm{d}x$$

where $I_{R/\theta}$ is the indicator function of the ball of radius R/θ. Then, the fully coupled system (7a)-(7b)-(14) corresponds to the system

$$\partial_{\boldsymbol{u}}\mathcal{E}(\boldsymbol{u},\boldsymbol{\xi},\theta) = 0, \tag{15a}$$

$$\dot{\boldsymbol{\xi}} \in \partial_{\boldsymbol{v}_{\boldsymbol{\xi}}}\mathcal{K}^*(\boldsymbol{u},\boldsymbol{\xi},\theta;\nabla\mathcal{S}(\boldsymbol{\xi},\theta)), \tag{15b}$$

$$\dot{\theta} \in \partial_{\boldsymbol{v}_\theta}\mathcal{K}^*(\boldsymbol{u},\boldsymbol{\xi},\theta;\nabla\mathcal{S}(\boldsymbol{\xi},\theta)). \tag{15c}$$

Note that equation (15c) corresponds exactly to (14) with the nonlinear term $\kappa\Delta(1/\theta)$ replacing $-\kappa\Delta\theta$. Indeed, the latter can be seen as a linearization of the former around some equilibrium temperature.

The variational structure of this system can be made even more explicit by eliminating the variable $\boldsymbol{u}$. Indeed, relation (15a) (or (7a) plus boundary conditions) defines a linear solution-map $\boldsymbol{\xi} \mapsto \phi(\boldsymbol{\xi}) = \boldsymbol{u}$. We can hence define

$$E(\boldsymbol{\xi},\theta) = \mathcal{E}(\phi(\boldsymbol{\xi}),\boldsymbol{\xi},\theta), \quad S = \mathcal{S}, \quad K^*(\boldsymbol{\xi},\theta;\boldsymbol{v}_{\boldsymbol{\xi}},\boldsymbol{v}_\theta) = \mathcal{K}^*(\phi(\boldsymbol{\xi}),\boldsymbol{\xi},\theta;\boldsymbol{v}_{\boldsymbol{\xi}},\boldsymbol{v}_\theta),$$

and let $\mathbf{y} = (\boldsymbol{\xi},\theta)$ in order to rewrite (15b)-(15c) as the *generalized gradient flow* [82]

$$\dot{\mathbf{y}} = \nabla K^*(\mathbf{y},\nabla S(\mathbf{y})).$$

Additional details on this perspective together with some related numerical discussion are provided in [7].

6.6. **Thermal control.** A vast majority of SMA actuators are driven by thermal control, usually in terms of an induced Joule effect. Some preliminary investigation on the possibility of controlling the SA model via thermal means is performed in [40]. For given temperatures $t \mapsto \theta(t)$, let us indicate with $\mathcal{S}(\theta)$ the set of all energetic solutions of the quasi-static evolution problem (7) (note that this set reduces to a point in case the thermomechanical coupling term is regularized). Then, one is interested in finding an *optimal control* θ and an *optimal solution* $(\boldsymbol{u}^*,\boldsymbol{\xi}^*) \in \mathcal{S}(\theta^*)$ for some cost functional J, namely

$$(\boldsymbol{u}^*,\boldsymbol{\xi}^*) \in \operatorname{Arg\,min}\{J(\boldsymbol{u},\boldsymbol{\xi},\theta) \mid (\boldsymbol{u},\boldsymbol{\xi}) \in S(\theta)\}.$$

By assuming suitable compatibility of the initial values and the controls, compactness of controls, and lower semicontinuity of the cost functional J, it is shown in [40] that the optimal control problem admits at least a solution.

7. **Residual plasticity.** Most SMAs experience the accumulation of permanent inelastic deformations under an increasing number of loading-unloading cycles. This fatigue-like accumulation causes a progressive degradation of the elastic properties of the materials and eventually saturates around on a maximal limiting value. This circumstance is responsible of a number of material failures compromising the efficiency of some SMA applications. The experimental evidence of fatigue effects has been reported for various alloys under different settings [3, 38, 119, 127] and a number of models including permanent inelastic strains have been recently proposed [24, 54, 70, 97]. An existence analysis for a SMA model including permanent plasticity is detailed in [69].

7.1. **Including permanent inelastic effects.** The SA model has been extended in [14, 15] in order to include permanent inelasticity and degradation effects. The extension consists in the introduction of a new internal variable $\boldsymbol{\xi}^{\rm pl}$ describing permanent inelastic strains. In particular, we assume that the inelastic strain $\boldsymbol{\xi}$ is linearly decomposed as $\boldsymbol{\xi} = \boldsymbol{\xi}^{\rm tr} + \boldsymbol{\xi}^{\rm pl}$ where $\boldsymbol{\xi}^{\rm tr}$ is activated by martensitic transformation whereas $\boldsymbol{\xi}^{\rm pl}$ corresponds to the permanent inelastic strain. The expression of the free energy ψ is then extended as follows

$$\begin{aligned}\psi(\boldsymbol{e}, \boldsymbol{\xi}^{\rm tr}, \boldsymbol{\xi}^{\rm pl}, \theta) &= c\theta(1-\log\theta) + \frac{1}{2}(\boldsymbol{e}-\boldsymbol{\xi}^{\rm tr}-\boldsymbol{\xi}^{\rm pl}){:}\mathbb{C}(\boldsymbol{e}-\boldsymbol{\xi}^{\rm tr}-\boldsymbol{\xi}^{\rm pl})\\ &+ \frac{1}{2}\boldsymbol{\xi}^{\rm tr}{:}\mathbb{H}^{\rm tr}\boldsymbol{\xi}^{\rm tr} + \frac{1}{2}\boldsymbol{\xi}^{\rm pl}{:}\mathbb{H}^{\rm pl}\boldsymbol{\xi}^{\rm pl} - \boldsymbol{\xi}^{\rm tr}{:}\mathbb{A}\boldsymbol{\xi}^{\rm pl} + f(\theta)|\boldsymbol{\xi}^{\rm tr}| + I(\boldsymbol{\xi}^{\rm tr}+\boldsymbol{\xi}^{\rm pl}). \qquad (16)\end{aligned}$$

In the latter, $\mathbb{H}^{\rm tr}$ and $\mathbb{H}^{\rm pl}$ are hardening tensors, referring to the two inelastic processes, respectively, and $\mathbb{A}$ encodes the (supposedly bilinear) coupling among the two. We shall always assume $\mathbb{A}^2 - \mathbb{H}^{\rm tr}{:}\mathbb{H}^{\rm pl} \leq 0$ so that the whole free energy is convex in $(\boldsymbol{\xi}^{\rm tr}, \boldsymbol{\xi}^{\rm pl})$. Note that the thermomechanical coupling term depends the transformation strain $\boldsymbol{\xi}^{\rm tr}$ only whereas the whole inelastic strain $\boldsymbol{\xi}^{\rm tr}+\boldsymbol{\xi}^{\rm pl}$ is bounded by the indicator function I.

The dissipative character of the model follows from prescribing $D(\dot{\boldsymbol{\xi}}^{\rm tr}, \dot{\boldsymbol{\xi}}^{\rm pl}) = I^*_K(\dot{\boldsymbol{\xi}}^{\rm tr}, \dot{\boldsymbol{\xi}}^{\rm pl})$ where the convex set K is given by

$$K = \{\boldsymbol{\zeta}^{\rm tr}, \boldsymbol{\zeta}^{\rm pl} \in \mathbb{R}^{3\times 3}_{\rm dev}\times\mathbb{R}^{3\times 3}_{\rm dev} \ : \ f(\boldsymbol{\zeta}^{\rm tr}, \boldsymbol{\zeta}^{\rm pl}) = |\boldsymbol{\zeta}^{\rm tr}| + \kappa|\boldsymbol{\zeta}^{\rm pl}| - R\}.$$

Here, an additional material parameter $\kappa \geq 0$ has been introduced for the sake of modulating the permanent inelastic effects. In [14] it is proved that these choices allow for the description of both saturated and unsaturated permanent inelastic effects as well as the degradation phenomenon. In particular, numerical evidence assessing the performance of the model both in uniaxial and biaxial tests and the relevance of the material parameters have been presented. Some validation with respect to available uniaxial tests is also assessed.

The analysis of the model has been performed in [39]. In particular, the well-posedness of both the constitutive and the quasi-static evolution problems (suitably regularized, see Subsection 4.4) is discussed and explicit convergence rates for the time-discrete approximations are provided. Moreover, it is rigorously proved by evolutionary Γ-convergence that the model reduces to the original SA model for $\kappa \to 0$ and to linearized elastoplasticity with linear kinematic hardening (and bound on the plastic strain) for $\kappa = R \to \infty$.

7.2. **Grain size effects.** In a recent series of papers it has been show that the emergence of permanent inelastic effect is correlated to the specific sizes of the crystals in a NiTi polycrystal [34, 35, 76]. Indeed, in the amorphous (non crystallized) phase or for grains of the size of 5-10 nm the material behaves approximately elastically even in the super-elastic temperature range. By increasing the grain size to approximately 20-50 nm (for instance by heat-induced recrystallization) the material shows super-elastic behavior instead. By further increasing grain size to 100-200 nm, plastic effects emerge. In [55] an explicit dependence of the free energy (16) on the local proportion $\phi \in [0,1]$ or recrystallized phase and the local average radius $g > 0$ of grains. The main ansatz here is that the material behaves as a mixture of elastic and inelastic compounds, depending on ϕ. More precisely, we have that the actual inelastic strain of the ϕ-crystallized body reads $\phi\boldsymbol{\xi}$ where $\boldsymbol{\xi}$ is the inelastic strain of the fully crystallized specimen. Moving from this, by scaling one assumes that the material parameters depend on ϕ and g as

$$\beta(\phi,g) = \phi\widehat{\beta}(g), \quad \mathbb{H}^{\mathrm{tr}}(\phi,g) = \frac{1}{\phi}\widehat{H}^{\mathrm{tr}}(g)\mathbf{1}_2, \quad \mathbb{H}^{\mathrm{pl}}(\phi,g) = \frac{1}{\phi}\widehat{H}^{\mathrm{pl}}(g)\mathbf{1}_2,$$
$$\mathbb{A}(\phi,g) = \frac{1}{\phi}\widehat{A}(g)\mathbf{1}_2, \quad \epsilon_L(\phi,g) = \phi\widehat{\epsilon}_{\mathrm{L}}(g), \quad \kappa(\phi,g) = \widehat{\kappa}(g), \quad R(\phi,g) = \phi\widehat{R}(g).$$

In particular, the above functions $\widehat{\beta}$, $\widehat{H}^{\mathrm{tr}}$, $\widehat{H}^{\mathrm{pl}}$, $\widehat{A}$, $\widehat{\epsilon}_{\mathrm{L}}$, $\widehat{\kappa}(g)$, and $\widehat{R}$ are chosen in such a way to fit tension experiments in terms of observable quantities (such as activation and threshold stresses at particular cycles) along with the classical Hall-Petch law

$$\sigma_\infty = \sigma_0 + \frac{k}{g^{1/2}}$$

ensuing that the difference between the final and the initial activation stress scales like $g^{-1/2}$.

Along with this provisions, in [55] it is proved that the model reproduces the passage from elastic to super-elastic to plastic regimes for increasing grain sizes as well as the plastic saturation and the degradation of the elastic behavior due to plasticization.

8. **Magnetic shape-memory effect.** The shape-memory alloys Ni_2MnGa, NiMnInCo, NiFeGaCo, FePt, FePd, among others, are called *magnetic* (MSMAs) as they feature ferromagnetic martensitic phases. These entails the possibility of obtaining large strains by martensitic-variant reorientation under the imposition of an external magnetic field. The resulting macroscopic effect is often referred to as *giant* magnetostrictive response for strains as large as 10% can be activated. This motivates a strong interest for these materials for innovative devices applications. For details on the magnetic shape-memory effect the reader is referred, with no claim of completeness, to [36, 61, 62, 75, 95, 126], see also the review in [63].

The SA model has been extended to include the ferromagnetism of the martensitic phases in [4, 5, 6, 21]. Within the single-crystal setting, we assume magnetic uniaxiality within a cubic-tetragonal system. Namely, we let the *easy axis* of magnetization of each of the three martensitic variants to be aligned with one of the three axes in $\mathbb{R}^3$ (the cubic-orthorombic system is discussed in [6]). Hence, we have that each proportion $\boldsymbol{p} \in S \subset \mathbb{R}^3$ features an *easy axis* of magnetization in direction $\boldsymbol{p}$.

Before going on, let us briefly review some literature on MSMA modeling. Early modeling contributions have been mainly focusing on the energy minimization mechanism. Among these, we shall minimally refer to [36, 93, 94, 126]. As for thermodynamically consistent models, one has to mention the contributions by [95, 96, 92]. Internal-variable models have been introduced by [57, 52] and [64, 65], see also [66, 80]. The later has been extended in order to encompass some more realistic magnetic response by [132]. Let us stressa that all MSMA models proposed so far deal with single crystals. Indeed MSMAs polycrystals, despite their relatively easier production process, are presently not yet exploited in real devices because of the observed significant drop in the observed magnetostrictive strain [31] and brittleness [122].

8.1. **Strong magnetic anisotropy.** Let us assume at first that the material presents a very strong magnetic anisotropy so that the actual magnetization of martensites is rigidly attached to the corresponding easy axes and no magnetization rotation actually takes place. The magnetization $\boldsymbol{m}$ is given by

$$\boldsymbol{m} = m_{\rm sat}\alpha\boldsymbol{p} \tag{17}$$

where $m_{\rm sat} > 0$ is the saturation magnetization. The *orientation* of the variants with respect to the easy axis will be determined by the scalar (signed) *magnetic-domain proportion* $\alpha \in [-1,1]$. This particularly entail that $|\boldsymbol{M}| = |m_{\rm sat}\alpha\boldsymbol{p}| \leq m_{\rm sat}|\alpha|\,|\boldsymbol{p}| \leq m_{\rm sat}$. Strong magnetic anisotropy is in large agreement with observations on Ni_2MnGa [95, 126].

8.2. **Magnetic Gibbs energy.** The constitutive relations for the model are derived from the specification of the Gibbs free energy density encompassing magnetism as well

$$G_{\rm mag}(\boldsymbol{\sigma},\boldsymbol{p},\theta,\boldsymbol{h},\alpha) := G(\boldsymbol{\sigma},\boldsymbol{\xi}(\boldsymbol{p}),\theta) + \frac{1}{2\delta}\alpha^2 + I_{[-1,1]}(\alpha) - \mu_0\boldsymbol{h}{\cdot}m_{\rm sat}\alpha\boldsymbol{p}. \tag{18}$$

The additional terms in the Gibbs energy encode the magnetic behavior of the material. The term $-\mu_0\boldsymbol{h}\cdot m_{\rm sat}\alpha\boldsymbol{p}$ is the classical *Zeeman energy* term $-\mu_0\boldsymbol{h}{\cdot}\boldsymbol{m}$. Note that $\boldsymbol{h}$ stands here for the *internal* magnetic field. Namely, $\boldsymbol{h}$ is the magnetic field which is actually experienced by the material when subjected to some (externally) applied field. In particular, $\boldsymbol{h}$ corresponds to the sum of the applied external field and the corresponding induced demagnetization field. The indicator function $I_{[-1,1]}$ constraints the signed domain proportion α to take values in $[-1,1]$ and $1/\delta$ is a user-defined (dimensionalized in MPa) hardening-like parameter modulating the tendency of magnetic domains to equilibrate at $\alpha = 0$. As temperature effects are not of interest here, we fix some suitable temperature θ^* (under the Curie temperature) such that field-induced reorientation of martensitic variants may take place. Correspondingly, β^* stands for the constant nonnegative value $\beta(\theta^*)$. Note that the Gibbs energy is invariant with respect to material symmetries [6].

Given the Gibbs energy (18), we classically derive the constitutive equations (1)-(2) as well as

$$\mu_0\boldsymbol{m} = -\partial_{\boldsymbol{h}}G_{\rm mag} = m_{\rm sat}\alpha\boldsymbol{p}, \tag{19a}$$

$$\boldsymbol{\zeta} \in \partial_{\boldsymbol{p}}G_{\rm mag} = -\boldsymbol{\sigma}{:}\boldsymbol{E} + \beta^*\partial_{\boldsymbol{p}}|\boldsymbol{\xi}(\boldsymbol{p})| + \mathbb{H}\boldsymbol{\xi}(\boldsymbol{p}){:}\boldsymbol{E} + \partial_{\boldsymbol{p}}I_S(\boldsymbol{p}) - \mu_0 m_{\rm sat}\alpha\boldsymbol{h}, \tag{19b}$$

$$g \in \partial_\alpha G_{\rm mag} = \delta^{-1}\alpha + \partial I_{[-1,1]}(\alpha) - \mu_0 m_{\rm sat}\boldsymbol{h}{\cdot}\boldsymbol{p}. \tag{19c}$$

Here, $g \in \mathbb{R}$ is the *thermodynamic force* associated with the internal variable α.

8.3. **Dissipation and constitutive relation.** We shall assume the dissipation to be given by $D = D(\dot{\boldsymbol{p}}) = R|\dot{\boldsymbol{p}}|$. In particular, we assume no dissipation in the magnetic-domain proportion α. This is of course disputable as the dissipation in α is, indeed, the only dissipative mechanism in simple ferromagnetic materials. Still, MSMA experiments show that, at small strains, the dissipation in α is negligible with respect to that in $\boldsymbol{p}$ [32, 64].

As the magnetic-domain proportion α is non-dissipative, we have that the thermodynamic force g vanishes. Hence, by solving relation (19c) for $g = 0$ one can obtain α as a function of $\boldsymbol{h}$ and $\boldsymbol{p}$. In particular, we have that $\alpha = \Pi_{[-1,1]}\big(\delta\mu_0 m_{\rm sat}\boldsymbol{h}\cdot\boldsymbol{p}\big) := \max\big\{-1, \min\big\{1, \delta\mu_0 m_{\rm sat}\boldsymbol{h}\cdot\boldsymbol{p}\big\}\big\}$ where $\Pi_{[-1,1]}$ denotes the projection onto $[-1,1]$. In other words, one can minimize out α from the Gibbs energy (18) in order to obtain a *reduced* Gibbs-energy density. The minimum is attained exactly at $\alpha = \Pi_{[-1,1]}\big(\delta\mu_0 m_{\rm sat}\boldsymbol{h}\cdot\boldsymbol{p}\big)$ so that

$$\begin{aligned} G_{\rm red}(\boldsymbol{\sigma},\boldsymbol{p},\theta,\boldsymbol{h}) &:= \min_{\alpha} G_{\rm mag}(\boldsymbol{\sigma},\boldsymbol{p},\theta,\boldsymbol{h},\alpha) \\ &= -\frac{1}{2}\boldsymbol{\sigma}{:}\mathbb{C}^{-1}{:}\boldsymbol{\sigma} - \boldsymbol{\sigma}{:}\boldsymbol{\xi}(\boldsymbol{p}) + F_{\rm SA}(\boldsymbol{p}) - F_{\rm mag}(\boldsymbol{h}\cdot\boldsymbol{p}). \end{aligned}$$

In the latter we have introduced the convex functions $F_{\rm SA}$ and $F_{\rm mag} \in C^{1,1}(\mathbb{R})$ as

$$\begin{aligned} F_{\rm mag}(r) &:= \frac{1}{2\delta}\min\Big\{(\delta\mu_0 m_{\rm sat} r)^2, 2|\delta\mu_0 m_{\rm sat} r| - 1\Big\} \quad \text{for all } r\in\mathbb{R} \\ F_{\rm SA}(\boldsymbol{p}) &:= \beta^*|\boldsymbol{\xi}(\boldsymbol{p})| + \frac{1}{2}\boldsymbol{\xi}(\boldsymbol{p}){:}\mathbb{H}\boldsymbol{\xi}(\boldsymbol{p})|^2 + I_S(\boldsymbol{p}). \end{aligned}$$

Hence, the right-hand side of relation (19b) reads $\mathrm{D}_{\boldsymbol{p}} F_{\rm mag}(\boldsymbol{h}\cdot\boldsymbol{p})$.

Given the above arguments, the final form of the constitutive equation problem reads

$$\partial D(\dot{\boldsymbol{p}}) + \partial F_{\rm SA}(\boldsymbol{p}) - \partial_{\boldsymbol{p}} F_{\rm mag}(\boldsymbol{h}\cdot\boldsymbol{p}) \ni \boldsymbol{\sigma}{:}\boldsymbol{E}. \tag{20}$$

In particular, the effective energy driving the evolution of $\boldsymbol{p}$ turns out to be the sum of a mechanical convex and a magnetic concave part.

8.4. **Existence results.** The strongly anisotropic case has been considered from the point of view of the existence of energetic solutions and their approximation in [6, 21]. In particular, given $t \mapsto (\boldsymbol{\sigma}(t), \boldsymbol{h}(t))$ suitably smooth one can prove that the constitutive relation (20) admits an energetic solution. The usual implicit Euler scheme serves well in order to prove such an existence result. Still, one has to record here the semiimplicit scheme

$$\partial D(\boldsymbol{p}^k - \boldsymbol{p}^{k-1}) + \partial F_{\rm SA}(\boldsymbol{p}^k) - \partial_{\boldsymbol{p}} F_{\rm mag}(\boldsymbol{h}(t^k)\cdot\boldsymbol{p}^{k-1}) \ni \boldsymbol{\sigma}(t^k){:}\boldsymbol{E}$$

which shows improved stability, as the nonmonotone term $-\partial_{\boldsymbol{p}} F_{\rm mag}$ is evaluated explicitly.

By suitably augmenting the constitutive equation by the nonlocal term $\partial V(\boldsymbol{\xi}(\boldsymbol{p}))$ (see (8)), the full quasi-static evolution problem (7a)+(7c)-(7d)+(20) also admits an energetic solution. This follows by observing that the nonmonotone magnetic coupling term is smooth, albeit nonlinear. Finally, the nonmagnetic SA model can be rigorously recovered by letting the parameter $\delta \to 0$ by using the evolutionary Γ-convergence theory for rate-independent processes [89]. This serves also as a cross validation of the magnetic extension of the SA model.

8.5. **Weak magnetic anisotropy.** By dropping the strong-anisotropy ansatz (17) one is forced to include the magnetization $\boldsymbol{m}$ in the list of state variables. This has been done in [22] in the case $\theta^* < \theta_*$ (that is, pure martensite at zero stress) for the total energy

$$E(t, \boldsymbol{u}, \boldsymbol{\xi}, \boldsymbol{m}) = \int_\Omega \psi(\boldsymbol{\varepsilon}(\boldsymbol{u}), \boldsymbol{\xi}, \theta^*) - \int_{\Gamma^{\rm tr}} \boldsymbol{g}\cdot\boldsymbol{u} + \frac{\mu_0}{2}\int_{\mathbb{R}^3} |\nabla v_{\boldsymbol{m}}|^2$$
$$- \mu_0 \int_\Omega \boldsymbol{h}(t)\cdot\boldsymbol{m} + \kappa_{\boldsymbol{m}} \int_\Omega |\nabla \boldsymbol{m}|^2 - \mu_0 \kappa_{\rm ani} \int_\Omega (\boldsymbol{m}\cdot\boldsymbol{p})^2 + V(\boldsymbol{\xi}(\boldsymbol{p}))$$

under the constraints

$$|\boldsymbol{m}| = m_{\rm sat}, \quad \mathrm{div}(-\mu_0 \nabla v_{\boldsymbol{m}} + \boldsymbol{m}\chi_\Omega) = 0 \ \text{ in } \mathbb{R}^3$$

where the first is nothing but magnetization saturation while the second is the Maxwell equation defining the *magnetostatic potential* $v_{\boldsymbol{m}}$ (χ_Ω is the characteristic function of Ω). The corresponding term in E is the *magnetostatic energy* term. The energy features also the *Zeeman term* $-\mu_0 \boldsymbol{h}\cdot\boldsymbol{m}$ and the *exchange energy* term, modulated by the constant $\kappa_{\boldsymbol{m}}$ [27]. The anisotropic term $-\mu_0\kappa_{\rm ani}\int_\Omega(\boldsymbol{m}\cdot\boldsymbol{p})^2$ is minimized when $\boldsymbol{m}$ is parallel to the easy axis $\boldsymbol{p}$. Finally, the nonlinear term $V(\boldsymbol{\xi}(\boldsymbol{p}))$ has been explicitly included in the energy in order to give rise to a scale effect with the aim of penalizing martensitic phase boundaries and possibly describing the occurrence of a specific twinning length scale.

By assuming the dissipation of the system in the form

$$D(\dot{\boldsymbol{p}}, \dot{\boldsymbol{m}}) = \int_\Omega R_{\boldsymbol{p}} |\dot{\boldsymbol{p}}| + \int_\Omega R_{\boldsymbol{m}} |\dot{\boldsymbol{m}}|$$

one can prove that there exist energetic solutions for the pair (E, D). Moreover, again by exploiting the general theory of [89] one can prove that by letting $R_{\boldsymbol{m}} \to \infty$ the model rigorously reduces to the purely mechanical one. On the other hand, by taking $R_{\boldsymbol{p}} \to \infty$ one obtains a specific micromagnetic model instead. Finally, by letting $R_{\boldsymbol{m}} \to 0$ one recovers the nondissipative-magnetics limit [22].

8.6. **Magnetic control.** The giant magnetostrictive behavior of MSMA provides the unprecedented possibility of activating devices at a distance by tuning an external magnetic field. A preliminary analysis in this direction is reported in [124] where an optimal control problem is considered. There, the admissible control is a time-dependent imposed magnetic field $t \mapsto \boldsymbol{h}(t)$ and the controllable quantities are the displacement $\boldsymbol{u}$ and the phase $\boldsymbol{p}$, which are energetic solutions of the corresponding quasi-static evolution model. Under suitable compactness assumptions, the existence of an optimal triplet of trajectories $(\boldsymbol{u}^*, \boldsymbol{p}^*, \boldsymbol{h}^*)$ minimizing a given cost functional under the constraint that $(\boldsymbol{u}^*, \boldsymbol{p}^*)$ is an energetic solution for $\boldsymbol{h}^*$ is proved. Due to the inherent nonsmoothness of the solution map $\boldsymbol{h} \mapsto (\boldsymbol{u}, \boldsymbol{p})$, necessary conditions for optimality seem particularly delicate and are presently not available.

9. **Thermal and electric couplings.** The models in [6, 21] has been recently extended in the direction of including thermal and electric couplings. By additionally assuming viscous dynamics (see Subsection 6.4), in [116] an extension of the SA model is introduced and the corresponding weak solvability is discussed. More

precisely, one is interested in describing the material via the extended free energy density

$$\psi(\boldsymbol{e},\boldsymbol{p},p,\theta,\boldsymbol{m},\boldsymbol{b},\nabla\boldsymbol{\xi},\nabla\boldsymbol{m}) = \psi_{\rm therm}(p,\theta,\boldsymbol{m}) + \psi_{\rm mech}(\boldsymbol{e},\boldsymbol{p}) + \psi_{\rm mag}(\boldsymbol{m},\boldsymbol{b}) \\ + \psi_{\rm coupl}(\boldsymbol{p},\boldsymbol{m}) + \psi_{\rm NL}(\nabla\boldsymbol{p},\nabla\boldsymbol{m}) + \psi_{\rm constr}(\boldsymbol{p},\boldsymbol{m}).$$

Here p is an additional internal variable, possibly to be related with the total proportion of the martensitic phase and $\boldsymbol{b}$ stands for magnetic induction. in particular, we choose

$$\begin{aligned}
\psi_{\rm therm}(p,\theta,\boldsymbol{m}) &= \alpha_0(\theta) + \alpha_1(\theta)\gamma(p) + \frac{a_0}{2}\theta|\boldsymbol{m}|^2,\\
\psi_{\rm mech}(\boldsymbol{e},\boldsymbol{p}) &= \frac{1}{2}(\boldsymbol{\varepsilon}-\boldsymbol{\xi}(\boldsymbol{p})):\mathbb{C}(\boldsymbol{\varepsilon}-\boldsymbol{\xi}(\boldsymbol{p})) + \frac{1}{2}\boldsymbol{\xi}(\boldsymbol{p}):\mathbb{H}\boldsymbol{\xi}(\boldsymbol{p}),\\
\psi_{\rm mag}(\boldsymbol{m},\boldsymbol{b}) &= \frac{1}{2\mu_0}|\boldsymbol{b}-\mu_0\boldsymbol{m}|^2,\\
\psi_{\rm coupl}(\boldsymbol{p},\boldsymbol{m}) &= \frac{b_0}{4}|\boldsymbol{m}|^4 - \kappa_{\rm ani}|\boldsymbol{m}\cdot\boldsymbol{p}|^2\\
\psi_{\rm NL}(\nabla\boldsymbol{p},\nabla\boldsymbol{m}) &= \frac{\kappa_{\boldsymbol{p}}}{2}|\nabla\boldsymbol{p}|^2 + \frac{\kappa_{\boldsymbol{m}}}{2}|\nabla\boldsymbol{m}|^2\\
\psi_{\rm constr}(\boldsymbol{\xi},\boldsymbol{m}) &= I_S(\boldsymbol{p}) + I_{[0,1]}(p) + I_{|\boldsymbol{m}|\leq m_{\rm sat}}(\boldsymbol{m}).
\end{aligned}$$

The term $\psi_{\rm therm}$ features a purely thermic term (of prescribed polynomial behavior), a latent heat term, and a thermo-magnetic coupling term ($a_0 > 0$) whereas $\psi_{\rm mech}$ is the quadratic part of the classical SA energy. The term $\psi_{\rm mag}$ describes magnetostatics and $\psi_{\rm coupl}$ represents magneto-mechanical couplings, with b_0, $\kappa_{\rm ani} > 0$, and $I_{[0,1]}$ is the indicator function of the interval $[0,1]$. Finally, $\psi_{\rm NL}$ and $\psi_{\rm constr}$ encode nonlocal effects and constraints on the variables.

The dissipation is assumed to be of viscous type, namely

$$D(\boldsymbol{p},\theta;\dot{\boldsymbol{p}},\dot{p},\dot{\boldsymbol{m}},\nabla\theta,\boldsymbol{e}) = D_{\boldsymbol{p}}(\dot{\boldsymbol{p}},\dot{p}) + \frac{d_{\boldsymbol{p}}}{2}|(\dot{\boldsymbol{p}},\dot{p})|^2 + D_{\boldsymbol{m}}(\dot{\boldsymbol{m}}) + \frac{d_{\boldsymbol{m}}}{2}|\dot{\boldsymbol{m}}|^2 \\ + \frac{1}{2}\mathbb{K}(\boldsymbol{p},p,\theta)|\nabla\theta|^2 + \frac{1}{2}\mathbb{S}(\boldsymbol{p},p,\theta)|\boldsymbol{e}|^2$$

where $D_{\boldsymbol{p}}$ and $D_{\boldsymbol{m}}$ are positively 1-homogeneous, $d_{\boldsymbol{p}}$, $d_{\boldsymbol{m}} > 0$ are viscosity coefficient $\mathbb{K}$ and $\mathbb{S}$ represent heat and electric conductivity and $\boldsymbol{e}$ is the electric field.

By assuming now the constitutive relations

$$\boldsymbol{\sigma} = \partial_{\boldsymbol{\varepsilon}}\psi, \quad \boldsymbol{h} = \partial_{\boldsymbol{b}}\psi, \quad s = -\partial_\theta\psi, \quad -\boldsymbol{q} = \partial_{\nabla\theta}D,$$

and $\boldsymbol{j} = \partial_{\boldsymbol{e}}D$, the model consists in the thermo-electro-mechanical system

$$\begin{aligned}
\text{entropy equation:} &\qquad \theta\dot{s} + \nabla\cdot\boldsymbol{q} = \partial_{(\dot{\boldsymbol{p}},\dot{\boldsymbol{m}},\boldsymbol{e})}D\cdot(\dot{\boldsymbol{p}},\dot{\boldsymbol{m}},\boldsymbol{e}),\\
\text{quasi-static equilibrium:} &\qquad \nabla\boldsymbol{\sigma} = \boldsymbol{0},\\
\text{internal variables evolution:} &\qquad \partial_{(\dot{\boldsymbol{p}},\dot{p},\dot{\boldsymbol{m}})}D + \partial_{(\boldsymbol{p},p,\boldsymbol{m})}\psi \ni \boldsymbol{0},\\
\text{eddy-current Maxwell's system:} &\qquad \dot{\boldsymbol{b}} + \nabla\times\boldsymbol{e} = \boldsymbol{0}, \quad \nabla\times\boldsymbol{h} = \boldsymbol{j}.
\end{aligned}$$

The basic idea of the model resides in the possibility of considering *smooth* function $\gamma(p)$ in the termal part of the energy (cfr. the original (5)). This allows to circumvent the thermodynamic (and analytic) obstruction mentioned in Subsection 6.3. The final outcome of the model corresponds to a generalization also of the classical Frémond model [46, 47] to complex martensitic structures and electromagnetism. Additionally, the model represents an extension of former contributions in thermoviscoelasticity and magnetostriction to the full coupling of effects. In particular, the present model can be related with that of [118] where, nonetheless, the phase descriptor $\boldsymbol{\xi}$ was not appearing. The present convexity assumption on the free energy allows fro a stronger solution notion with respect to that of [118]. The reader is referred to [116] for a thorough discussion. By referring to the discussion in Subsection 6.4 one has however to mention that here the thermomechanical coupling in the material is not assumed to be linear in θ. Along this same line of thought, the reader is referred to [115] where a thermoviscoelastic evolution problem with general nonlinear thermal coupling (but no phase change nor magnetism) is considered.

By assuming smoothness on nonlinearities and suitable nondegeneracy for α_0, $\mathbb{K}$, and $\mathbb{S}$ one can perform an enthalpy-like trasformation allowing for the passage to the limit in a suitable time discretization. This entails in particular the existence of a weak solution [116].

Acknowledgement. This research has been partially supported by The ERC-FP7-Ideas-StG Grant #200497 *Biosma* and by the IMATI-CNR, Pavia.

REFERENCES

[1] T. Aiki. A model of 3D shape memory alloy materials. *J. Math. Soc. Japan*, 57 (2005) 903–933.
[2] M. Arndt, M. Griebel, T. Roubíček. Modelling and numerical simulation of martensitic transformation in shape memory alloys. *Contin. Mech. Thermodyn.*, 15 (2003) 463–485.
[3] M. Arrigoni, F. Auricchio, V. Cacciafesta, L. Petrini, R. Pietrabissa. Cyclic effects in shape-memory alloys: a one-dimensional continuum model. *J. Phys. IV France*, 11 (2001) 577–582.
[4] F. Auricchio, A.-L. Bessoud, A. Reali, U. Stefanelli. Macroscopic modeling of magnetic shape memory alloys. *Oberwolfach Reports*, 14 (2010) 771–773.
[5] F. Auricchio, A.-L. Bessoud, A. Reali, U. Stefanelli. A three-dimensional phenomenological models for magnetic shape memory alloys. *GAMM-Mitt.*, 34 (2011) 90–96.
[6] F. Auricchio, A.-L. Bessoud, A. Reali, U. Stefanelli. A phenomenological model for the magneto-mechanical response of single-crystal Magnetic Shape Memory Alloys. Preprint IMATI-CNR, 3PV13/3/0, 2013.
[7] F. Auricchio, E. Boatti, A. Reali, U. Stefanelli. The GENERIC formulation of coupled thermomechanical response in shape-memory alloys. In preparation, 2013.
[8] F. Auricchio, E. Bonetti. A new "flexible" 3D macroscopic model for shape memory alloys. *Discrete Contin. Dyn. Syst. Ser. S*, 6 (2013) 2:277–291.
[9] F. Auricchio, J. Lubliner. A uniaxial model for shape-memory alloys. *Internat. J. Solids Structures*, 34 (1997) 3601–3618.
[10] F. Auricchio, A. Mielke, U. Stefanelli. A rate-independent model for the isothermal quasi-static evolution of shape-memory materials. *Math. Models Meth. Appl. Sci.*, 18 (2008) 125–164.
[11] F. Auricchio, L. Petrini. Improvements and algorithmical considerations on a recent three-dimensional model describing stress-induced solid phase transformations. *Internat. J. Numer. Methods Engrg.*, 55 (2002) 1255–1284.
[12] F. Auricchio, L. Petrini. A three-dimensional model describing stress-temperature induced solid phase transformations. Part I: Solution algorithm and boundary value problems. *Internat. J. Numer. Meth. Engrg.*, 61 (2004) 807–836.
[13] F. Auricchio, L. Petrini. A three-dimensional model describing stress-temperature induced solid phase transformations. Part II: Thermomechanical coupling and hybrid composite applications. *Internat. J. Numer. Meth. Engrg.*, 61 (2004) 716–737.
[14] F. Auricchio, A. Reali, U. Stefanelli. A three-dimensional model describing stress-induces solid phase transformation with residual plasticity. *Int. J. Plasticity*, 23 (2007) 207–226.
[15] F. Auricchio, A. Reali, U. Stefanelli. A phenomenological 3D model describing stress-induced solid phase transformations with permanent inelasticity. In *Topics on Mathematics for Smart Systems*, B. Miara, G. Stavroulakis, and V. Valente (eds.), 1–14. World Sci. Publ., Hackensack, NJ, 2007.

[16] F. Auricchio, A. Reali, U. Stefanelli. A macroscopic 1D model for shape memory alloys including asymmetric behaviors and transformation-dependent elastic properties. *Comput. Methods Appl. Mech. Engrg.*, 198 (2009) 1631–1637.

[17] F. Auricchio, U. Stefanelli. Well-posedness and approximation for a one-dimensional model for shape memory alloys. *Math. Models Meth. Appl. Sci.*, 15 (2005) 9:1301–1327.

[18] K. Bhattacharya. *Microstructures of Martensites*. Oxford Series on Materials Modeling, Oxford University Press, Oxford, 2003.

[19] V. Berti, M. Fabrizio, D. Grandi. Phase transitions in shape memory alloys: A non-isothermal Ginzburg-Landau model. *Phys. D*, 239 (2010) 95–102.

[20] V. Berti, M. Fabrizio, D. Grandi. Hysteresis and phase transitions for one-dimensional and three-dimensional models in shape memory alloys. *J. Math. Phys.*, 51 (2010) 062901.

[21] A.-L. Bessoud, U. Stefanelli. Magnetic shape memory alloys: Three-dimensional modeling and analysis. *Math. Models Meth. Appl. Sci.*, 21 (2011) 1043–1069.

[22] A.-L. Bessoud, M. Kružík, U. Stefanelli. A macroscopic model for magnetic shape memory alloys. *Z. Angew. Math. Phys.*, 64 (2013) 2:343–359.

[23] H. Brézis. *Operateurs Maximaux Monotones et Semi-Groupes de Contractions dans les Espaces de Hilbert*. Math Studies, Vol.5, North-Holland, Amsterdam/New York, 1973.

[24] Z. Bo, D. Lagoudas. Thermomechanical modeling of polycrystalline SMAs under cyclic loading. Part III: evolution of plastic strains and two- way shape memory effect. *Int. J. Engrg. Sci.*, 37 (1999) 1175–1203.

[25] E. Bonetti. Global solvability of a dissipative Frémond model for shape memory alloys. I. Mathematical formulation and uniqueness. *Quart. Appl. Math.*, 61 (2003) 759–781.

[26] M. Brokate, J. Sprekels. *Hysteresis and phase transitions*. Applied Mathematical Sciences, 121. Springer-Verlag, New York, 1996.

[27] W. F. Brown, Jr.. *Magnetoelastic interactions*. Springer, Berlin, 1966.

[28] N. Bubner, J. Sokołowski, J. Sprekels. Optimal boundary control problems for shape memory alloys under state constraints for stress and temperature. *Numer. Funct. Anal. Optim.*, 19 (1998) 489–498.

[29] P. Colli. Global existence for the three-dimensional Frémond model of shape memory alloys. *Nonlinear Anal.*, 24 (1995) 1565–1579.

[30] P. Colli, M. Frémond, A. Visintin. Thermo-mechanical evolution of shape memory alloys. *Quart. Appl. Math.*, 48 (1990) 31–47.

[31] S. Conti, M. Lenz, M. Rumpf. Macroscopic behaviour of magnetic shape-memory polycrystals and polymer composites. *Mater. Sci. Engrg. A*, 481-482 (2008) 351–355.

[32] B. D. Cullity, C. D. Graham. *Introduction to magnetic materials*. Second ed., Wiley., 2008.

[33] F. Daghia, M. Fabrizio, D. Grandi. A non isothermal Ginzburg-Landau model for phase transitions in shape memory alloys. *Meccanica*, 45 (2010) 797–807.

[34] R. Delville, B. Malard, J. Pilch, P. Šittner, D. Schryvers. Microstructure changes during non-conventional heat treatment of thin NiTi wires by pulsed electric current studied by transmission electron microscopy. *Acta Mater.*, 58 (2010) 4503–4515.

[35] R. Delville, B. Malard, J. Pilch, P. Šittner, D. Schryvers. Transmission electron microscopy study of microstructural evolution in nanograined Ni-Ti microwires heat treated by electric pulse. *Solid State Phenom.*, 172–174 (2011) 682–687.

[36] A. DeSimone, R. D. James. A constrained theory of magnetoelasticity. *J. Mech. Phys. Solids*, 50 (2020) 283–320.

[37] T. W. Duerig, A. R. Pelton (eds.). *SMST-2003 Proceedings of the International Conference on Shape Memory and Superelastic Technology Conference*, ASM International, 2003.

[38] J. Dutkiewicz. Plastic deformation of CuAlMn shape-memory alloys. *J. Mat. Sci.*, 29 (1994) 6249–6254.

[39] M. Eleuteri, L. Lussardi, U. Stefanelli. A rate-independent model for permanent inelastic effects in shape memory materials. *Netw. Heterog. Media*, 6 (2011) 145–165.

[40] M. Eleuteri, L. Lussardi, U. Stefanelli. Thermal control of the Souza-Auricchio model for shape memory alloys. *Discrete Cont. Dyn. Syst.-S*, 6 (2013) 369–386.

[41] V. Evangelista, S. Marfia, E. Sacco. Phenomenological 3D and 1D consistent models for shape-memory alloy materials. *Comput. Mech.*, 44 (2009) 405–421.

[42] V. Evangelista, S. Marfia, E. Sacco. A 3D SMA constitutive model in the framework of finite strain. *Internat. J. Numer. Methods Engrg.*, 81 (2010) 761–785.

[43] F. Falk, Model free energy, mechanics and thermodynamics of shape memory alloys. *Acta Metal.* 28 (1990) 1773–1780.

[44] F Falk. P Konopka. Three-dimensional Landau theory describing the martensitic phase transformation of shape-memory alloys. *J. Phys.: Condens. Matter*, 2 (1990) 61–77.

[45] G. Francfort, A. Mielke. Existence results for a class of rate-independent material models with nonconvex elastic energies. *J. Reine Angew. Math.*, 595 (2006) 55–91.

[46] M. Frémond. Matériaux à mémoire de forme. *C. R. Acad. Sci. Paris Sér. II Méc. Phys. Chim. Sci. Univers Sci. Terre*, 304 (1987) 239–244.

[47] M. Frémond. *Non-Smooth Thermomechanics*. Springer-Verlag, Berlin, 2002.

[48] M. Frémond, S. Miyazaki. *Shape Memory Alloys*. CISM Courses and Lectures, vol. 351, Springer-Verlag, 1996.

[49] M. Frémond, E. Rocca. A model for shape memory alloys with the possibility of voids. *Discrete Contin. Dyn. Syst.* 27 (2010) 4:1633–1659.

[50] S. Frigeri, P. Krejčí, U. Stefanelli. Quasistatic isothermal evolution of shape memory alloys *Math. Models Meth. Appl. Sci.*, 21 (2011) 12:2409–2432.

[51] S. Frigeri, U. Stefanelli. Existence and time-discretization for the finite-strain Souza-Auricchio constitutive model for shape-memory alloys. *Contin. Mech. Thermodyn.*, 24 (2012) 63–77.

[52] J.-Y. Gauthier, C. Lexcellent, A. Hubert, J. Abadie, N. Chaillet. Magneto-thermo-mechanical modeling of a magnetic shape memory alloy Ni-Mn-Ga single crystal. *Ann. Solid Struct. Mech.*, 2 (2001) 19–31.

[53] S. Govindjee, C. Miehe. A multi-variant martensitic phase transformation model: Formulation and numerical implementation. *Comput. Methods Appl. Mech. Engrg.*, 191 (2001) 215–238.

[54] S. Govindjee, E. P. Kasper. A shape memory alloy model for uranium- niobium accounting for plasticity. *J. Intelligent Mat. Syst. Struct.*, 8 (1997) 815–823.

[55] D. Grandi, U. Stefanelli. Modeling microstructure-dependent inelasticity in shape-memory alloys. Preprint IMATI-CNR 13PV13/11/0, 2013.

[56] D. Helm, P. Haupt, Shape memory behaviour: modelling within continuum thermomechanics. *Intern. J. Solids Struct.*, 40 (2003) 827–849.

[57] L. Hirsinger, C. Lexcellent. Internal variable model for magneto-mechanical behaviour of ferromagnetic shape memory alloys Ni-Mn-Ga. *J. Phys. IV*, 112 (2003) 977–980.

[58] K.-H. Hoffmann, M. Niezgódka, Z. Songmu. Existence and uniqueness of global solutions to an extended model of the dynamical developments in shape memory alloys. *Nonlinear Anal.*, 15 (1990) 977–990.

[59] K.-H. Hoffmann, D. Tiba. Control of a plate with nonlinear shape memory alloy reinforcements. *Adv. Math. Sci. Appl.*, 7 (1997) 427–436.

[60] K.-H. Hoffmann, A. Żochowski. Control of the thermoelastic model of a plate activated by shape memory alloy reinforcements. *Math. Methods Appl. Sci.*, 21 (1998) 589–603.

[61] R. D. James, M. Wuttig. Magnetostriction of martensite. *Phil. Mag. A,* 77 (1998) 1273–1299.

[62] H. E. Karaca, I. Karaman, B. Basaran, Y. I. Chumlyakov, H. J. Maier. Magnetic field and stress induced martensite reorientation in NiMnGa ferromagnetic shape memory alloy single crystals. *Acta Mat.*, 54 (2006) 233–245.

[63] J. Kiang, L. Tong. Modelling of magneto-mechanical behaviour of NiMnGa single crystals. *J. Magn. Magn. Mater.*, 292 (2005) 394–412.

[64] B. Kiefer. *A phenomelogical model for magnetic shape memory alloys*. PhD Thesis, Texas A&M, 2006.

[65] B. Kiefer, D. C. Lagoudas. Modeling the coupled strain and magnetization response of magnetic shape memory alloys under magnetomechanical loading. *J. Intell. Mater. Syst. Struct.*, 20 (2009) 143–170.

[66] B. Kiefer, H. Karaca, D. C. Lagoudas, I. Karaman. Characterization and modeling of the magnetic field-induced strain and work output in Ni_2MnGa magnetic shape memory alloys. *J. Magn. Magn. Mater.*, 312 (2007) 164–175.

[67] P. Krejčí, U. Stefanelli. Existence and nonexistence for the full thermomechanical Souza-Auricchio model of shape memory wires. *Math. Mech. Solids*, 16 (2011) 349–365.

[68] P. Krejčí, U. Stefanelli. Well-posedness of a thermo-mechanical model for shape memory alloys under tension. *M2AN Math. Model. Numer. Anal.*, 44 (2010) 6:1239–1253.

[69] M. Kružík, J. Zimmer. A model of shape memory alloys taking into account plasticity. *IMA J. Appl. Math.*, 76 (2011) 1:193–216.

[70] D. C. Lagoudas, P. Entchev. Modeling of transformation-induced plas- ticity and its effect on the behavior of porous shape memory alloys. Part I: constitutive model for fully dense SMAs. *Mech. Mat.*, 36 (2004) 865–892.

[71] D. C. Lagoudas, P. B. Entchev, P. Popov, E. Patoor, L. C. Brinson, X. Gao. Shape memory alloys, Part II: Modeling of polycrystals. *Mech. Materials*, 38 (2006) 391–429.

[72] E. Lee. Elastic-plastic deformation at finite strains. *J. Appl. Mech*, 36 (1969) 1–6.

[73] V. I. Levitas. Thermomechanical theory of martensitic phase transformations in inelastic materials. *Intern. J. Solids Struct.*, 35 (1998) 889–940.

[74] Ch. Lexcellent. *Shape-Memory Alloys Handbook*. Wiley, 2013.

[75] A. A. Likhachev, K. Ullakko. Magnetic-field-controlled twin boundaries motion and giant magneto-mechanical effects in NiMnGa shape memory alloy. *Phys. Lett. A*, 275 (200) 142–151.

[76] B. Malard, J. Pilch, P. Šittner, R. Delville, C. Curfs. In situ investigation of the fast microstructure evolution during electropulse treatment of cold drawn NiTi wires. *Acta Mater.*, 59 (2011) 1542–1556.

[77] A. Mainik, A. Mielke. Existence results for energetic models for rate-independent systems, *Calc. Var. Partial Differential Equations*, 22 (2005) 73–99.

[78] M. Maraldi, L. Molari, D. Grandi. A non-isothermal phase-field model for shape memory alloys: numerical simulations of superelasticity and shape memory effect under stress- controlled conditions. *J. Intelligent Mat. Syst. Struct.*, 23 (2012) 1083–1092.

[79] M. Maraldi, L. Molari, D. Grandi. A macroscale, phase-field model for shape memory alloys with non-isothermal effects: influence of strain-rate and environmental conditions on the mechanical response. *Acta Mat.*, 60 (2012) 179–191.

[80] C. Miehe, B. Kiefer, D. Rosato. An incremental variational formulation of dissipative magnetostriction at the macroscopic continuum level. *Internat. J. Solids Struct.*, 48 (2011) 1846–1866.

[81] A. Mielke. Evolution of rate-independent systems. in *Handbook of Differential Equations, Evolutionary Equations*, C. Dafermos, E. Feireisl (eds.), Elsevier, 2005, 461–559.

[82] A. Mielke. Formulation of thermoelastic dissipative material behavior using GENERIC. *Contin. Mech. Thermodyn.*, 23 (2011) 3:233-256.

[83] A. Mielke. On thermodynamically consistent models and gradient structures for thermoplasticity. *GAMM Mitt.*, 34 (2011) 1:51-58.

[84] A. Mielke, L. Paoli, A. Petrov. On existence and approximation for a 3D model of thermally induced phase transformations in shape-memory alloys. *SIAM J. Math. Anal.*, 41 (2009) 1388–1414.

[85] A. Mielke, L. Paoli, A. Petrov, U. Stefanelli. Error estimates for space-time discretizations of a rate-independent variational inequality. *SIAM J. Numer. Anal.*, 48 (2010) 1625–1646.

[86] A. Mielke, L. Paoli, A. Petrov, U. Stefanelli. Error bounds for space-time discretizations of a 3d model for shape-memory materials. In *IUTAM Symposium on Variational Concepts with Applications to the Mechanics of Materials*, K. Hackl (ed.), 185–197. Springer, 2010. Proceedings of the IUTAM Symposium on Variational Concepts, Bochum, Germany, Sept. 22–26, 2008.

[87] A. Mielke, A. Petrov. Thermally driven phase transformation in shape-memory alloys, *Adv. Math. Sci. Appl.*, 17 (2007) 667–685.

[88] A. Mielke, F. Rindler. Reverse approximation of energetic solutions to rate-independent processes. *NoDEA Nonlinear Differential Equations Appl.*, 16 (2009) 17–40.

[89] A. Mielke, T. Roubíček, U. Stefanelli. Γ-limits and relaxations for rate-independent evolutionary problems. *Calc. Var. Partial Differential Equations*, 31 (2008) 3:387–416.

[90] A. Mielke, U. Stefanelli. Linearized plasticity is the evolutionary Γ-limit of finite plasticity. *J. Eur. Math. Soc. (JEMS)*, 15 (2013) 3:923–948.

[91] A. Mielke, F. Theil. On rate-independent hysteresis models. *NoDEA Nonlinear Diff. Equations Applications*, 11 (2004) 151–189.

[92] S. J. Murray, M. Marioni, P. G. Tello, S. M. Allen, R. C. O'Handley. Giant magnetic-field-induced strain in Ni-Mn-Ga crystals: experimental results and modeling. *J. Magn. Magn. Mater.*, 226–230 (2001) 945–947.

[93] S. J. Murray, S. M. Allen, R. C. O'Handley, T. A. Lograsso. Magnetomechanical performance and mechanical properties of Ni-Mn-Ga ferromagnetic shape memory alloys. In *SPIE Proceedings*, 3992 (2000) 387.

[94] S. J. Murray, R. C. O'Handley, S. M. Allen. Model for discontinuous actuation of ferromagnetic shape memory alloy under stress. *J. Appl. Phys.* 89 (2000) 1295–1301.

[95] R. C. O'Handley. Model for strain and magnetization in magnetic shape-memory alloys, *J. Appl. Phys.*, 83 (1998) 3263–3270.

[96] R. C. O'Handley, S. J. Murray, M. Marioni, H. Nembach, S. M. Allen. Phenomenology of giant magnetic-field-induced strain in ferromagnetic shape-memory materials. *J. Appl. Phys.*, 87 (200) 4712–4717.

[97] A. Paiva, M. A. Savi, A. M. B. Braga, P. M. C. L. Pacheco. A constitutive model for shape memory alloys considering tensile-compressive asymmetry and plasticity. *Int. J. Solids Struct.*, 42 (2005) 3439–3457.

[98] I. Pawłow, W. M. Zajaczkowski. Global existence to a three-dimensional non-linear thermoelasticity system arising in shape memory materials. *Math. Methods Appl. Sci.*, 28 (2005) 407–442.

[99] L. Paoli, A. Petrov. Global existence result for phase transformations with heat transfer in shape memory alloys. Preprint Arxiv 1104.5408, 2011.

[100] L. Paoli, A. Petrov. Existence result for a class of generalized standard materials with thermomechanical coupling. Preprint Arxiv 1111.2436, 2011.

[101] L. Paoli, A. Petrov. Thermodynamics of multiphase problems in viscoelasticity. *GAMM-Mitt.*, 35 (2012) 1:75–90.

[102] L. Paoli, A. Petrov. Global existence result for thermoviscoelastic problems with hysteresis. *Nonlinear Anal. Real World Appl.*, 13 (2012) 2:524–542.

[103] L. Paoli, A. Petrov. Solvability for a class of generalized standard materials with thermomechanical coupling. *Nonlinear Anal. Real World Appl.*, 14 (2013) 1:111–130.

[104] I. Pawłow, A. Żochowski. A control problem for a thermoelastic system in shape memory materials, Sūrikaisekikenkyūsho Kōkyūroku, No. 1210 (2011), 8–23, Free boundary problems (Japanese) (Kyoto, 2000).

[105] B. Peultier, T. Ben Zineb, E. Patoor. Macroscopic constitutive law for SMA: Application to structure analysis by FEM. *Materials Sci. Engrg. A*, 438-440 (2006) 454–458.

[106] P. Popov, D. C. Lagoudas. A 3-D constitutive model for shape memory alloys incorporating pseudoelasticity and detwinning of self-accommodated martensite. *Int. J. Plasticity*, 23 (2007) 1679–1720.

[107] B. Raniecki, Ch. Lexcellent. R_L models of pseudoelasticity and their specification for some shape-memory solids. *Eur. J. Mech. A Solids*, 13 (1994) 21–50.

[108] S. Reese, D. Christ. Finite deformation pseudo-elasticity of shape memory alloys – Constitutive modelling and finite element implementation. *Int. J. Plasticity*, 24 (2008) 455–482.

[109] F. Rindler. Optimal control for nonconvex rate-independent evolution processes. *SIAM J. Control Optim.*, 47 (2008) 2773–2794.

[110] F. Rindler. Approximation of rate-independent optimal control problems. *SIAM J. Numer. Anal.*, 47 (2009) 3884–3909.

[111] T.Roubíček. Models of microstructure evolution in shape memory alloys. In *Nonlinear Homogenization and its Appl.to Composites, Polycrystals and Smart Materials*, P. Ponte Castaneda, J. J. Telega, B. Gambin (eds.), NATO Sci. Series II/170, Kluwer, Dordrecht, 2004, 269–304.

[112] T. Roubíček. Rate-independent processes in viscous solids at small strains. *Math. Methods Appl. Sci.*, 32 (2009) 7:825–862.

[113] T. Roubíček. Thermodynamics of rate-independent processes in viscous solids at small strains. *SIAM J. Math. Anal.*, 42 (2010) 1:256–297.

[114] T. Roubíček. Approximation in multiscale modelling of microstructure evolution in shape-memory alloys. *Cont. Mech. Thermodynam.*, 23 (2011) 491–507.

[115] T. Roubíček. Nonlinearly coupled thermo-visco-elasticity. *NoDEA Nonlinear Differential Equations Appl.*, 20 (2013) 3:1243–1275.

[116] T. Roubíček, U. Stefanelli. Magnetic shape-memory alloys: thermomechanical modeling and analysis. Preprint IMATI-CNR 6PV13/0/0, 2013.

[117] T. Roubíček, G. Tomassetti. Thermodynamics of shape-memory alloys under electric current. *Z. Angew. Math. Phys.*, 61 (2010) 1:1–20.

[118] T. Roubíček, G. Tomassetti. Phase transformations in electrically conductive ferromagnetic shape-memory alloys, their thermodynamics and analysis. *Arch. Ration. Mech. Anal.*, 210 (2013) 1–43.

[119] P. Šittner, Y. Hara, M. Tokuda. Experimental study on the thermoelastic martensitic transformation in shape memory alloy polycrystal induced by combined external forces. *Metall. Materials Trans.*, 26A (1995) 2923–2935.

[120] J. Sokołowski, J. Sprekels. Control problems with state constraints for shape memory alloys. *Math. Methods Appl. Sci.*, 17 (1994) 943–952.

[121] A. C. Souza, E. N. Mamiya, N. Zouain. Three-dimensional model for solids undergoing stress-induced tranformations. *Eur. J. Mech. A Solids*, 17 (1998) 789–806.

[122] A. Sozinov, A. A. Likhachev, N. Lanska, K. Ullakko. Giant magnetic-field-induced strain in NiMnGa seven-layered martensitic phase. *Appl. Phys. Lett.*, 80 (2002) 1746–1748.

[123] U. Stefanelli, Analysis of a thermomechanical model for shape memory alloys. *SIAM J. Math. Anal.*, 37 (2005) 130–155.

[124] U. Stefanelli. Magnetic control of magnetic shape-memory single crystals. *Phys. B*, 407 (2012) 1316–1321.

[125] P. Thamburaja, L. Anand. Polycrystalline shape-memory materials: effect of crystallographic texture. *J. Mech. Phys. Solids*, 49 (2001) 709–737.

[126] R. Tickle, R. D. James. Magnetic and magnetomechanical properties of Ni_2MnGa. *J. Magn. Magn. Mater.*, 195 (1999) 627–638.

[127] R. A. Vandermeer, J. C. Ogle, W. G. Jr. Northcutt. A phenomenological study of the shape memory effect in polycrystalline Uranium-Niobium alloys. *Metal. Trans A*, 12A (1981) 733–741.

[128] A. Visintin. *Differential Models of Hysteresis*, volume 111 of *Applied Mathematical Sciences*, Springer, Berlin, 1994.

[129] G. Wachsmuth. Optimal control of quasistatic plasticity with linear kinematic hardening, Part I: Existence and discretization in time. *SIAM J. Control Optim.*, 50 (2012) 5:2836–2861.

[130] G. Wachsmuth. Optimal control of quasistatic plasticity with linear kinematic hardening, part II: Regularization and differentiability. Preprint SPP1253-119, 2011.

[131] G. Wachsmuth. Optimal control of quasistatic plasticity with linear kinematic hardening, part III: Optimality conditions. Preprint SPP1253-119, 2011.

[132] J. Wang, P. Steinmann. A variational approach towards the modelling of magnetic field-induced strains in magnetic shape memory alloys. *J. Mech. Phys. Solids*, 60 (2012) 1179–1200.

[133] S. Yoshikawa, I. Pawłow, W. M. Zajaczkowski. Quasi-linear thermoelasticity system arising in shape memory materials. *SIAM J. Math. Anal.*, 38 (2007) 1733–1759.

[134] J. Zimmer. Global existence for a nonlinear system in thermoviscoelasticity with nonconvex energy. *J. Math. Anal. Appl.*, 292 (2004) 589–604.

Received XXXXXXX; revised XXXXXXX.

E-mail address: diego.grandi@univie.ac.at
E-mail address: ulisse.stefanelli@univie.ac.at